

Utah State University

DigitalCommons@USU

All Graduate Theses and Dissertations

Graduate Studies

8-2018

On Thermal Bowing of Concrete Sandwich Wall Panels with Flexible Shear Connectors

Fray Pozo
Utah State University

Follow this and additional works at: <https://digitalcommons.usu.edu/etd>



Part of the [Construction Engineering and Management Commons](#)

Recommended Citation

Pozo, Fray, "On Thermal Bowing of Concrete Sandwich Wall Panels with Flexible Shear Connectors" (2018). *All Graduate Theses and Dissertations*. 7133.

<https://digitalcommons.usu.edu/etd/7133>

This Thesis is brought to you for free and open access by the Graduate Studies at DigitalCommons@USU. It has been accepted for inclusion in All Graduate Theses and Dissertations by an authorized administrator of DigitalCommons@USU. For more information, please contact digitalcommons@usu.edu.



ON THERMAL BOWING OF CONCRETE SANDWICH WALL PANELS

WITH FLEXIBLE SHEAR CONNECTORS

by

Fray Pozo

A thesis submitted in partial fulfillment
of the requirements for the degree

of

MASTER OF SCIENCE

in

Civil Engineering

Approved:

Marc Maguire, Ph.D.
Major Professor

Joseph Caliendo, Ph.D.
Committee Member

Paul Barr, Ph.D.
Committee Member

Mark R. McLellan, Ph.D.
Vice President for Research and
Dean of the School of Graduate Studies

UTAH STATE UNIVERSITY
Logan, Utah

2018

Copyright © Fray Pozo 2018

All Rights Reserved

ABSTRACT

On Thermal Bowing of Concrete Sandwich Wall Panels

With Flexible Shear Connectors

by

Fray Pozo, Master of Science

Utah State University, 2018

Major Professor: Dr. Marc Maguire
Department: Civil and Environmental Engineering

Thermal bowing, often referred as bulging or out-of-plane wall deflection, is a common issue on sandwich panel walls caused by a temperature differential between a building interior temperature and the environment. The stresses caused by temperature changes in concrete members are widely known in the practice of bridge design, but not on sandwich wall panels. For sandwich wall panel applications, it is common to have non-composite panels when the designer expects a high temperature gradient, what yields a less economical design, but reduces the bowing. If a designer opts for a different composite behavior, the calculation of the thermal bowing is often estimated using classical mechanics equations, which do not consider composite action and yield incorrect results most of the time, yet conservative.

This project aimed to validate current assumptions regarding the heat flow in sandwich wall panels and to perform a parametric study of panels subject to thermal loads, varying the concrete layer thickness, panel length, type of shear connector and

separation using a commercial finite element analysis software; to develop equations, based on the parametric study, to predict thermal bowing on sandwich panels at the service limit state, so structural engineers have a more accurate way to predict thermal deflections. The equations developed with this method were applied to the out-of-plane stability analysis of sandwich wall panels to know the performance, issues and possible flaws of the code related to thermal gradients considerations in design. This study concluded that current design practices either underestimate, in the case of multiplying the classical mechanics values by the reported degree of composite behavior, or overestimate the real value of bowing, by using classical mechanics. A method for determining the percentage of composite action and compute bowing was developed and recommendations addressing the importance of this type of loading were given.

(101 pages)

PUBLIC ABSTRACT

On Thermal Bowing of Concrete Sandwich Wall Panels with Flexible Shear Connectors

Fray Pozo

Thermal bowing, often referred as bulging or out-of-plane wall deflection, is a common issue on sandwich panel walls caused by a temperature differential between a building interior temperature and the environment. The stresses caused by temperature changes in concrete members are widely known in the practice of bridge design, but not on sandwich wall panels. For sandwich wall panel applications, it is common to have non-composite panels when the designer expects a high temperature gradient, what yields a less economical design, but reduces the bowing.

This project aimed to validate current assumptions regarding the heat flow in sandwich wall panels and to perform a parametric study of panels subject to thermal loads, varying the concrete layer thickness, panel length, type of shear connector and separation using a commercial finite element analysis software. This study concluded that current design practices either underestimate, in the case of multiplying the classical mechanics values by the reported degree of composite behavior, or overestimate the real value of bowing, by using classical mechanics. A method for determining the percentage of composite action and compute bowing was developed and recommendations addressing the importance of this type of loading were given.

ACKNOWLEDGMENTS

The author acknowledges the MESCyT (Ministry of Higher Education, Science and Technology in Dominican Republic) for granting him a scholarship to pursue a master's degree at Utah State University.

The author also wants to express his deepest appreciation to Dr. Marc Maguire, for allowing him to be part of this research project and for all the guidance, support and patience through this process which helped him to stay focused and motivated.

Fray Francisco Pozo Lora

CONTENTS

	Page
ABSTRACT.....	iii
PUBLIC ABSTRACT	v
ACKNOWLEDGMENTS	vi
LIST OF TABLES	ix
LIST OF FIGURES	x
LIST OF SYMBOLS AND NOTATION.....	xiii
CHAPTER	
1. INTRODUCTION	1
1.1 Background	1
1.2 Objectives.....	2
1.3 Outline.....	2
2. LITERATURE REVIEW	3
2.1 Introduction	3
2.2 Sandwich Panels Composition.....	3
2.2.1 Typical Configurations	3
2.2.2 Insulation.....	4
2.2.3 Shear Connectors	4
2.3 Composite Action.....	5
2.4 Thermal Efficiency.....	7
2.5 Thermal Bowing.....	10
3. EXPERIMENTAL PROGRAM	16
3.1 Introduction	16
3.2 Full-scale test set up	16
3.3 Experimental Results.....	18
3.3.1 Material Testing Results	18
3.3.2 Full-scale Testing Results	19
3.4 Conclusions	21

4. PARAMETRIC ANALYSIS	22
4.1 Introduction	22
4.2 Finite Element Analysis	22
4.2.1 Beam–Spring Model	22
4.2.2 Shell–Spring Model	23
4.3 Validation of the Shell-Spring Model	23
4.4 Parametric Study	25
4.4.1 Effect of Panel Stiffness.....	25
4.4.2 Effect of Panel Length	28
4.4.3 Effect of distance between wythes centroid.....	31
4.4.4 Effect of temperature	34
4.4.5 Effect of concrete properties	35
4.5 Holmberg and Plem Equation, FEA and PCI Equation Comparison.....	36
4.6 Estimation of the percentage of composite action (PCA)	41
4.7 Conclusions	42
5. SERVICIABILITY ANALYSIS	44
5.1 Introduction	44
5.2 Sandwich Wall Panels with Out-of-Plane Bending	44
5.3 P- δ Analysis of Uncracked SWPs	45
5.4 Computation of Forces and deformations on Sandwich Wall panels	46
6. CONCLUSIONS.....	49
6.1 Full Scale Testing.....	49
6.2 Parametric Analysis.....	49
6.3 Serviceability Analysis.....	50
6.4 Future Research.....	50
REFERENCES	52
APPENDICES	55
Appendix A.....	56
Appendix B.....	61
Appendix C.....	67

LIST OF TABLES

Table		Page
4-1	Difference between FEA and equation (2-3) for a 323 panel.....	39
4-2	Difference between FEA and equation (4-1) for a 3-3-8 panel.....	40
4-3	Percentage differential between FEA and equation (2-3) for a 323 panel	40
4-4	Percentage differential between FEA and equation (4-1) for a 3-3-8 panel.....	40

LIST OF FIGURES

Figure		Page
2-1	Concrete Sandwich Panel Wall ((Olsen et al., 2017)	4
2-2	Shear Connectors Samples (Naito et al., 2011)	5
2-3	Composite Action on Concrete Sandwich Panels	6
2-4	Composite Action Behavior on Sandwich Panel with Temperature Differential.....	7
2-5	Heat flow on a sandwich panel wall.....	9
2-6	Typical panel support conditions (Leabu, 1960)	11
2-7	Thermal load effect on sandwich panel (Holmberg & Plem, 1965)	13
3-1	Sandwich Panel Cross-Section	16
3-2	Connector and reinforcement layout on sandwich wall panel.....	17
3-3	Location of thermocouples on sandwich panel – (a) General View, (b) Zoom at one quarter of the panel length (three thermocouples), (c) Zoom at mid-span (four thermocouples)	18
3-4	Load/Connector vs. Deflection CF 3in Model 23	19
3-5	Temperature variation on sandwich panel.....	20
3-6	Effect of temperature differential on sandwich panel bowing.....	20
4-1	Load versus deflection for "HK-2" Panel.....	24
4-2	Temperature differential versus deflection for full-scale panel test and FEA.....	24
4-3	Effect of Panel Stiffness on Out-of-Plane Deflection (left) and Connector Rotation (right) of a 3-2-3 Panel	26

Figure	Page
4-4	Effect of Panel Stiffness on maximum Connector Shear Force (left) and Axial Force (right) of a 3-2-3 Panel.....26
4-5	Effect of Panel Stiffness on Heated Wythe (OW) Stress, Tensile (left) and Compressive (right) of a 3-2-3 Panel.....27
4-6	Effect of Panel Stiffness on Unheated Wythe (IW) Stress, Tensile (left) and Compressive (right) of a 3-2-3 Panel.....27
4-7	Effect of Panel Length on Deflection28
4-8	Effect of Panel Length on Connector Maximum Rotation (left), and Maximum Slip (right)29
4-9	Effect of Panel Length on maximum Connector Shear Force (left) and Axial Force (right) of a 3-2-3 Panel.....29
4-10	Effect of Panel Length on Heated (Outer) Wythe Stress, Tensile (left) and Compressive (right) of a 3-2-3 Panel30
4-11	Effect of Panel Length on Unheated (inner) Wythe Stress, Tensile (left) and Compressive (right) of a 3-2-3 Panel30
4-12	Effect of distance between wythes centroid on thermal bowing, non-uniform wythe's variation (left) and uniform wythe's variation (right)31
4-13	Effect of Distance "d" on tensile stress of panels with unequal wythes.....32
4-14	Effect of Distance "d" on tensile stress of panels with equal wythes.32
4-15	Effect of Distance "d" on connector forces of panels with unequal wythes33
4-16	Effect of distance "d" on connector forces of panels with equal wythes.....33
4-17	Effect of temperature on deflection (left) and slip (right) of a 15 ft. long by 8 ft. wide panel with a 323 configuration34

Figure		Page
4-18	Effect of temperature on tensile stress of heated (left) and unheated (right) wythes of a 15 ft. long by 8 ft. wide panel with a 323 configuration.....	34
4-19	Effect of temperature on connector shear (left) and axial (right) forces of a 15 ft. long by 8 ft. wide panel with a 323 configuration.....	35
4-20	Effect of coefficient of thermal expansion on bowing	36
4-21	Effect of change in compressive strength on outer wythe tensile stress (left) and inner wythe tensile stress (right).....	37
4-22	Effect of change in compressive strength on connector shear force.....	37
4-23	Comparison of different bowing computation equations and FEA.....	39
5-1	Example of moment amplification	45
A.1-1	Panel subjected to a temperature differential	57

LIST OF SYMBOLS AND NOTATION

- $b =$ Width of the sandwich panel (cm)
 $d =$ Thickness of the wythe subjected to the thermal load
 $E =$ Modulus of Elasticity (kg/cm²)
 $I =$ Fully Composite Moment of Inertia of the panel section (cm⁴)
 $i =$ Sum of the moments of Inertia of the two individual wythes (cm⁴)
 $\chi = \sqrt{2kb/EcAc}$
 $k =$ Panel stiffness (kg/cm²/cm)
 $l =$ Length of the panel (cm)
 $l_o = \sqrt[4]{\frac{Ei}{2kb}}$
 $M_o = \frac{1}{2} \frac{\mu \times \Delta t \times EI}{d} \times \beta^2$
 $t =$ Thermal gradient of the whole panel (deg C)
 $\Delta t =$ Thermal gradient of a single wythe (deg C)
 $x =$ Abscissa (cm), as shown on Figure 2-6
 $\alpha^2 = 2Ar^2/I$
 $\beta^2 = 1 - \alpha^2$
 $\lambda = l\sqrt{2}/4l_o$
 $\mu =$ Coefficient of thermal expansion (cm \times C⁻¹ / cm)
 $\xi = x\sqrt{2}/2l_o$
 $\varphi =$ Relative displacement of the wythes (cm)
 $\varphi_1 = \cos(\xi) \cdot \cosh(\xi)$
 $\varphi_3 = \sin(\xi) \cdot \sinh(\xi)$
 $\varphi_i^0 = \varphi_i(\lambda)$
 $\psi = \varphi_1^0 (\varphi_2^0 \times \varphi_4^0) - \varphi_3^0 (\varphi_2^0 \times \varphi_4^0)$
 $\psi_1 = (\varphi_2^0 - \varphi_4^0)/\psi$
 $\psi_3 = (\varphi_2^0 + \varphi_4^0)/\psi$

CHAPTER 1

INTRODUCTION

1.1 Background

When the energy and economic crises of the 1970's struck the United States, the need of conserving energy became one of the priorities of the country, practically forcing the congress to pass a legislation requiring states to develop energy standards for new buildings. Concrete sandwich all panels (CSWPs), were the ideal solution to those problems, since they were already advertised as structural and thermally efficient. The structural portion of CSWPs generally consist of two layers of concrete (wythes) and one layer of foam in the middle (insulation). The wythes are tied together using shear connectors, which gives PCSPs a certain degree of composite behavior – non-composite, partially composite or fully-composite – depending on the type of connector and spacing used. CSWPs can also, be designed as load-bearing or non-load-bearing elements.

The stresses caused by temperature changes in concrete members are widely known in the practice of civil engineering. In certain situations, these are as important as live and dead load stresses and may cause concrete cracking. For CSWPs applications, it is common to have non-composite panels when the designer expects a high temperature gradient, what yields a less economical design, but reduces the bowing. If a designer opts for a different composite behavior, the calculation of the thermal bowing is often estimated using classical mechanics equations, which do not consider composite action and yield incorrect results most of the time, yet conservative.

1.2 Objectives

The goals of this research were: to perform a parametric study of panels subjected to thermal loads, varying the wythe's thickness, panel length, type of shear connector and separation; to test full-scale PCSPs with different connector types and separation, while having a 3-2-3 configuration (wythe-foam-wythe), and conventional reinforcing #4 bars spaced sixteen inches on center, each way and both wythes. Another objective was to develop equations, based on the parametric study and the testing results, to predict thermal bowing on sandwich panels at the service state, so engineers have a more accurate way to predict thermal deflections.

1.3 Outline

The research presented in this thesis starts with a literature review and comparison of the current methods used to predict thermal bowing on concrete sandwich wall panels. This is followed by the description of the experimental set up and results of three PCSPs subjected to thermal-gradient-type loads. The next chapter summarizes the modeling techniques and assumptions to be used in the parametric study; it also contains the model validation for both thermal and mechanical loads based on the previous tests results. The following chapter consists of a parametric study of PCSPs using a 3D finite element model using a commercial finite element software; a comparison of the results with methods mentioned in the literature review and the experimental results. Equations for bowing prediction are also developed using these results. The last chapter provides a summary of the research, conclusions, and recommendations.

CHAPTER 2

LITERATURE REVIEW

2.1 Introduction

This chapter briefly explain the composition of concrete sandwich panels, behavior, thermal efficiency, and deflection prediction when subjected to thermal loads.

2.2 Sandwich Panels Composition

Concrete sandwich wall panels, usually have three components: reinforced concrete layers, shear connectors and an insulation layer (Collins, 1954), as shown in Figure 2-1. The reinforcement of the wythes can be rebar, welded-wire or prestressing strands (Losch et al., 2011), and the connectors can be made of solid concrete pieces, steel or FRP composite connectors (Olsen, Al-Rubaye, Sorensen, & Maguire, 2017). Solid concrete wall panels and CSWPs differ in many things, but the two fundamental aspects are: flexural behavior and thermal efficiency. Solid walls have a higher flexural and axial capacity than sandwich walls, but they possess a poor thermal performance.

2.2.1 Typical Configurations

The market has a wide variety of sandwich panel configurations available. For tilt-up walls, the external wythe and insulation usually vary from 2” to 3”, and the interior wythe 6” or thicker. These panels are usually called by their thicknesses —e. g., 3–2–5, which means 3” external wythe, 2” insulation and 5” internal wythe. Precast panels have more variations, in addition of having a tilt-up configuration, they can combine hollow core or double-tee sections with foam and a non-structural wythe (Naito et al., 2011).

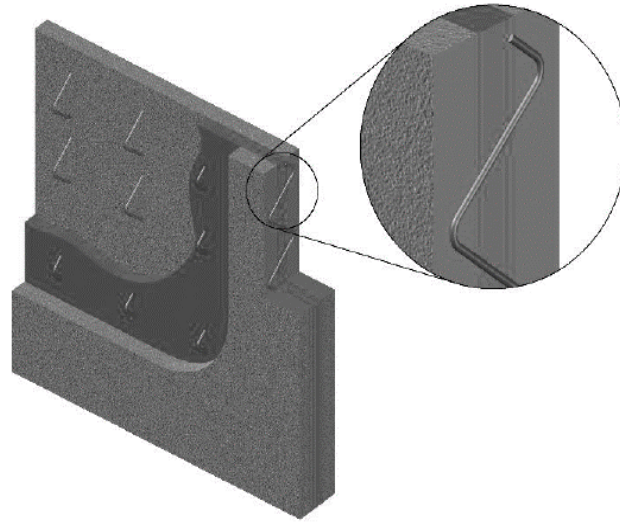


Figure 2-1 Concrete Sandwich Panel Wall ((Olsen et al., 2017)

2.2.2 Insulation

The most common types of foam insulation used in CSWPs are three: expanded polystyrene (EPS), extruded expanded polystyrene (XPS or XEPS), and polyisocyanurate (PIMA) (Naito et al., 2011). Their use frequency and thermal conductivity normally decreases from EPS to PIMA, while their cost, strength and density increase from EPS to XPS (PCI, 2010).

2.2.3 Shear Connectors

There are many types of shear connectors in the market, the most popular are the carbon and glass fiber ties, and steel ties, as shown in Figure 2-2. The first group provides the best thermal performance, while the second generate thermal bridging, and increase heat transmittance (Naito et al., 2011). Thermal bridging forms in CSWPs with steel ties because these ties have the highest thermal conductivity among all components, allowing heat to locally “by-pass” the insulation layer, creating a thermal gradient (McCall, 1985).

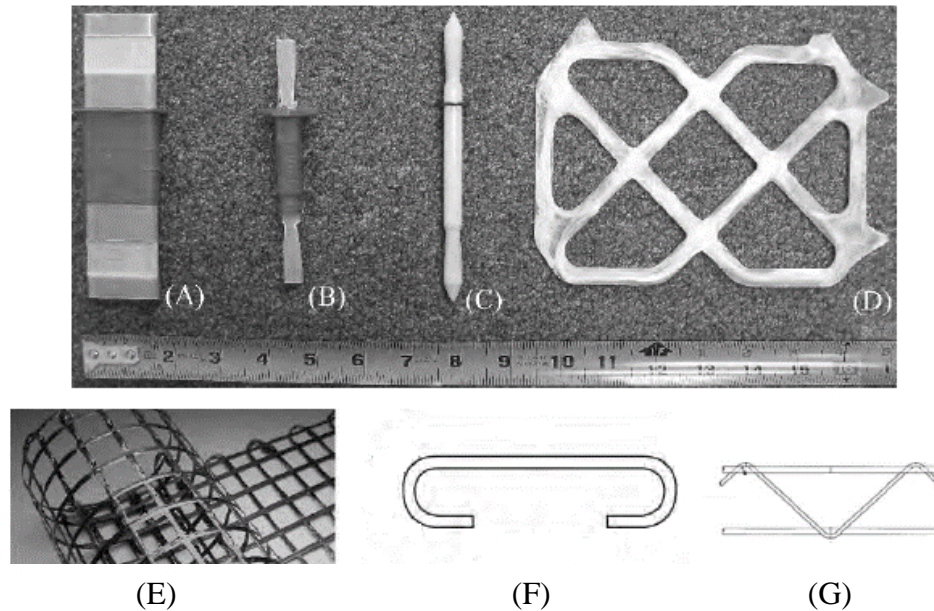


Figure 2-2 Shear Connectors Samples (Naito et al., 2011)

2.3 Composite Action

Composite action is often described as the degree to which two or more bodies act together to resist the stresses caused by external loads (Olsen et al., 2017). Consider a sandwich panel wall of two wythes and an insulation layer. Three cases are considered for a uniformly loaded panel respect to the interfaces between the insulation layer and the wythes: no friction between the layers, and hence no shear transfer; “rugged” surfaces, what means partial shear transfer; and no slip between the surfaces, which gives full shear transfer, as shown on Figure 2-3 (foam is ignored for clarity).

When a sandwich panel is subjected to transverse loads, the panel with no shear transfer capacity will behave as three separate members with relative slip free to occur between the them (Figure 2-3 b). This theoretically happens when pin-connectors are used (Figure 2-2 B and C).

When partially composite connectors are used (Figure 2-2 A and D), sliding can still occur, but it is restricted because of the shear transfer between the wythes, as shown on Figure 2-3 c. This interaction between the wythes increases the flexural capacity of the section but makes the panel susceptible to deformations due to thermal gradients.

The third case corresponds to a fully composite panel (Figure 2-3 d), which in theory has no slip between the interfaces, and behave as a single element. This behavior is easily achieved providing steel connectors (Figure 2-2 E-G), but decreases thermal efficiency drastically (PCI, 2010).

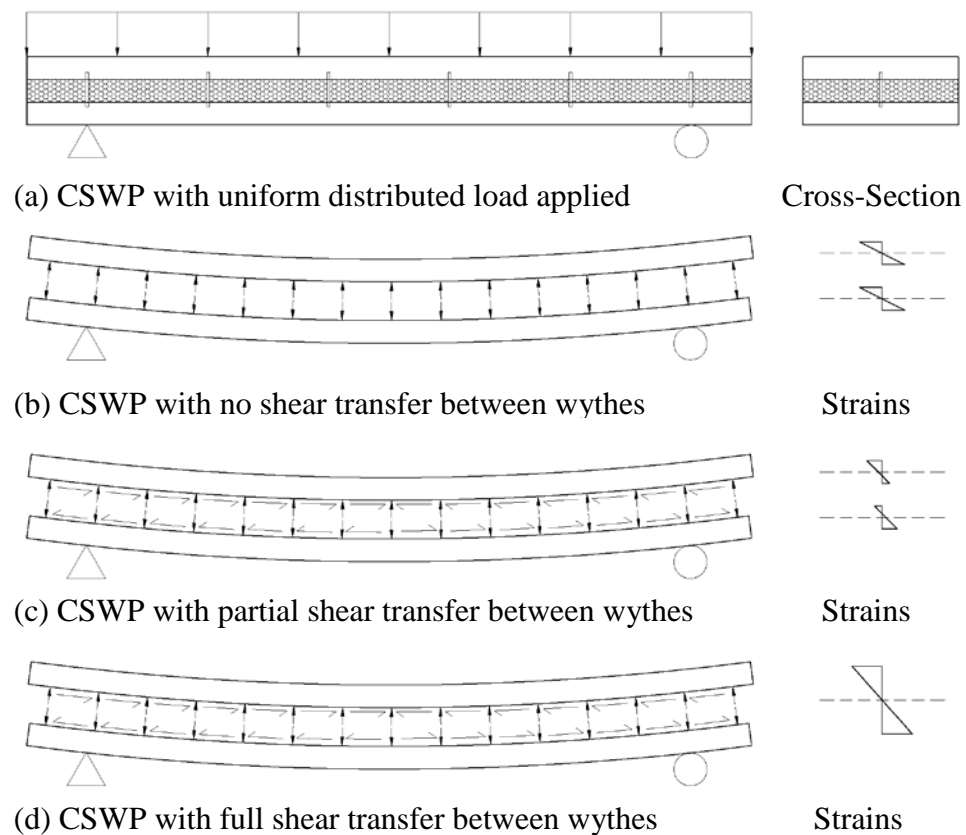


Figure 2-3 Composite Action on Concrete Sandwich Panels

On the other hand, if the panel is subjected to a temperature differential, the behavior is different. For the panel with no shear transfer between the two surfaces, the deflection is non-existent and therefore only one wythe expands or contracts. When shear connectors are introduced, the panel deflects, and the magnitude of stresses and deformations depend on the connecting medium stiffness, the dimensions of the member, etc., as shown on Figure 2-4. This deformation is due to the internal redundancy that connectors provide to the concrete layers and hence, the wythes bends instead of elongate.

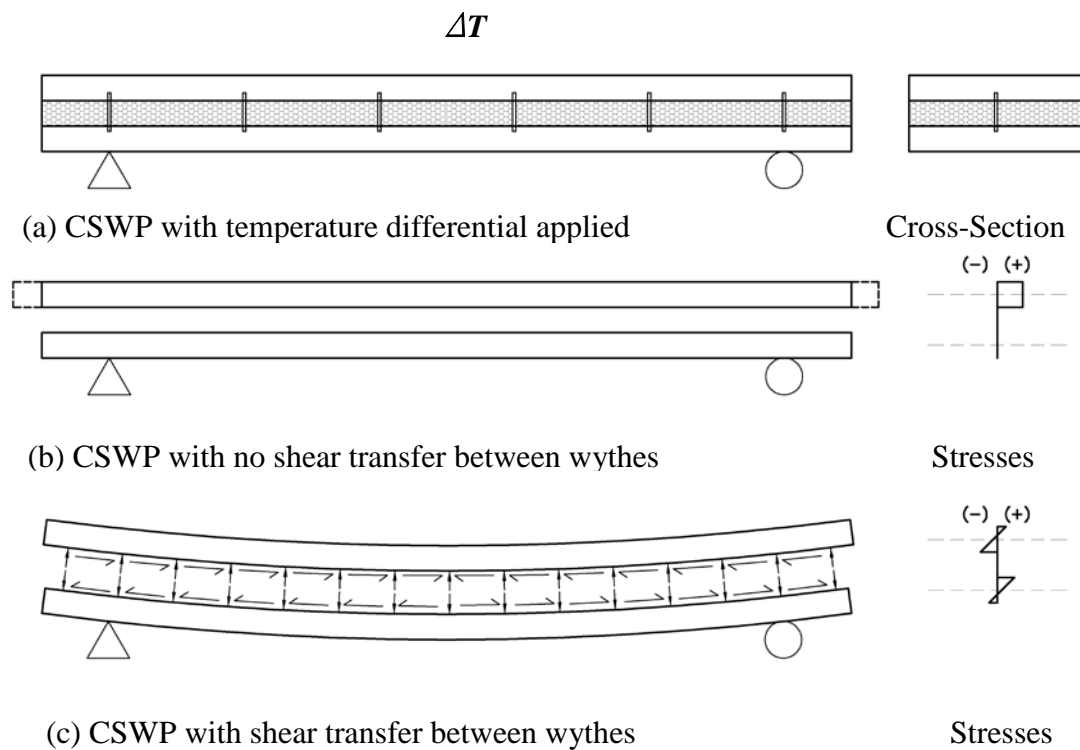


Figure 2-4 Composite Action Behavior on Sandwich Panel with Temperature Differential

2.4 Thermal Efficiency

Since the invention of sandwich panels, one of their main goal has been to be thermally efficient, and with codes and standards increasing the energy conservation requirements almost every cycle, the need of designing thermally efficient sandwich-type buildings has become one of the main tasks for architectural, civil and mechanical engineering practitioners.

When the environment or the building heating system increases surface temperature of CSWPs in normal dry condition, the heat tends to flow through the exposed wythe with almost no resistance but blocked off when it reaches the insulation portion of the panel, provided FRP ties are used. However, when metallic or solid block connectors penetrate the foam to join the wythes, the thermal performance decreases due to thermal bridging (McCall, 1985). In the case of wythes with higher moisture, the thermal conductance increases, generating a unsatisfactory and unpredictable performance (Balik & Barney, 1985).

Many researchers have studied the thermal design and performance of precast concrete members and buildings. Balik & Barney (1985), outlined the fundamentals involved in thermal design and assessment of buildings according to standards. They found out that concrete mass, insulation thickness, glass area, and controlled ventilation on affect the heat transmittance (U) values of precast members with different materials surface and properties. They also indicated the fact that seasons affect thermal gradients on buildings and concrete thermal resistance (R).

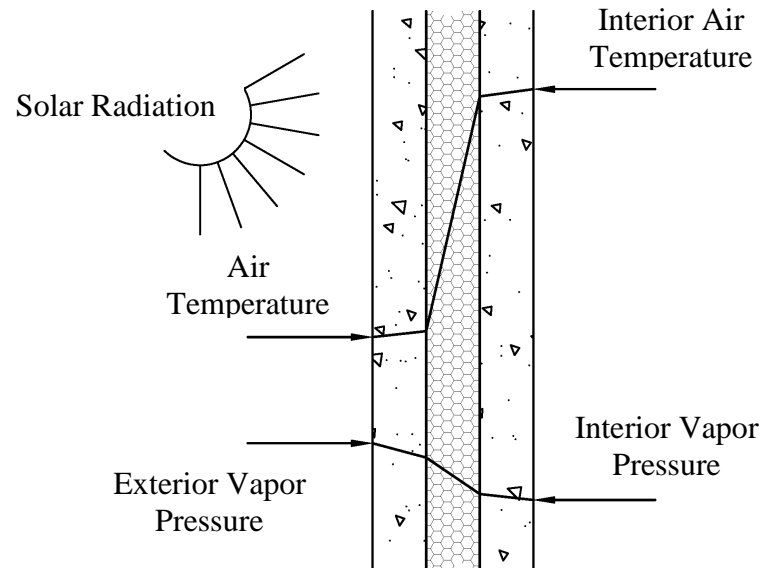


Figure 2-5 Heat flow on a sandwich panel wall

McCall (1985), discussed the necessary steps for calculating the total thermal resistance, thermal gradients, and the vapor pressure gradient of concrete sandwich panels (see Figure 2-5). This researcher addressed the need to consider: the effect of thermal bridging when calculating the U-value; reducing steel ties to increase thermal efficiency; and the effect of CSWP components densities when calculating the thermal transmittance.

Einea, Salmon, Tadros, & Culp (1997), tested the thermal efficiency of four 4ft square panels, two of them with FRP connectors, one with a steel truss and the other with concrete ribs. They determined that panels with FRP bent bars have a thermal efficiency of 75 to 88 % higher than a panel with concrete solid connectors and 11 to 19% higher than panels with steel truss connectors. They also suggested further investigation on the topic due to the specimen sizes and use of lifting anchors in the panel wythes.

Lee & Pessiki (2004), analytically investigated the thermal performance of three-wythe CSWPs, focusing on how the pattern of solid concrete strips and blocks affects the thermal resistance of the panel. They found the following differences in performance: ASHRAE Handbook method to calculate the R-value is inaccurate for three-wythe panels; the performance is better than the two-wythe panels; and that concrete wythe thickness does not play an important role on the thermal resistance of panels, irrespectively of the number of wythes.

Sorensen, Dorafshan, & Maguire (2017), investigated the common locations of heat loss on CSWPs. These researchers found multiple locations of thermal bridging on building envelopes. These spots include wall openings, where precaster usually cast a solid border around, wall penetrations, lifting points, panel to panel connections, etc. They suggested that engineers should take into account these places when detailing sandwich-type buildings, so thermal bridging reduces to a minimum.

2.5 Thermal Bowing

Thermal bowing, often referred as bulging or out-of-plane deflection, is a common issue on sandwich panel walls caused by a temperature differential. Bowing is an old problem, but not many researchers have investigated the issue. Leabu (1960), investigated common problems that affect the performance of precast wall panels. He stated that temperature differential affects more CSWPs than it does to precast foam, light weight or regular concrete walls. He suggested to compute the panel curvature using classical mechanics and considering two support conditions. This is the method suggested by the PCI Handbook (2010) for computing bowing.

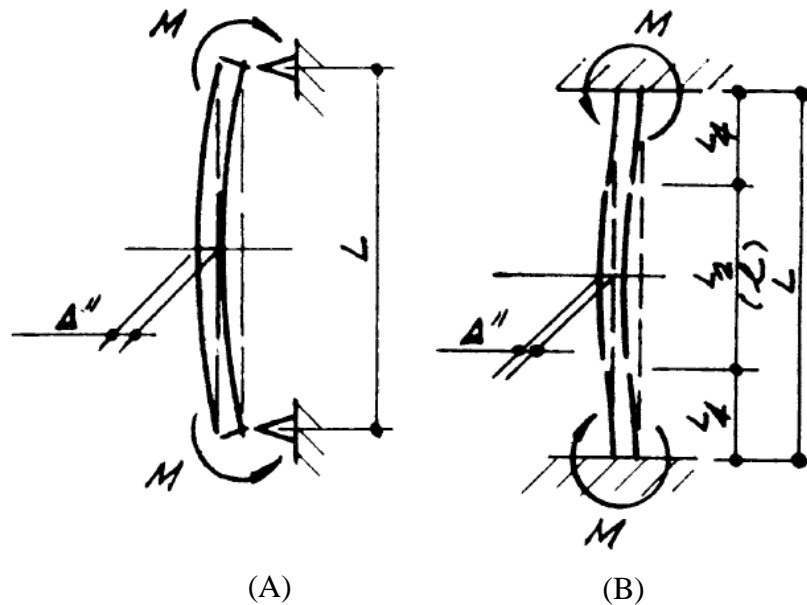


Figure 2-6 Typical panel support conditions (Leabu, 1960)

The first case corresponds to wall modeled as a pinned-pinned beam with moments at supports generated by the thermal gradient, as shown on Figure 2-6A, which represents a non-load bearing panel that spans between columns with only two supports. The second case is a fixed-fixed beam with equivalent moment at supports generated by the temperature differential (see Figure 2-6B), which emulates the roof or floor acting as a support.

Support condition 1:

$$\Delta_1 = \frac{c \times \delta T \times L^2}{8d} \quad (2-1)$$

Support condition 2:

$$\Delta_2 = \frac{c \times \delta T \times L^2}{32d} \quad (2-2)$$

Where:

$c =$ *Coefficient of thermal expansion (in $\times F^{-1}$ / in)*

$\delta T =$ *Difference of temperature between the outside and inside (deg F)*

$L =$ *Length of the panel (in)*

$d =$ *Effective depth of panel, distance between center of gravity of outer and inner faces (in)*

$\Delta =$ *Deflection at mid-span (in)*

The researcher also acknowledged that no experimental research was conducted to verify the values these equations yield, but the deflections computed typically correlate with the field observations. He also pointed that in some cases the thermal gradient cannot explain the behavior of the panels alone, and moisture differences and curing shrinkage could cause panel curvature. For these reasons, the CSWP and its connections should account for lateral panel movement, ductility and strength.

Granholm 1949 (as cited in Holmberg & Plem, 1965), developed a method for calculating stresses and deformations on composite wood beams and columns. The method was extended to sandwich panels by Holmberg & Plem (1965). The main assumption is that the panel to have two wythes tied together by a continuous connector, which is responsible of transferring the loads between the two concrete layers when it deflects. Their method included different loading types, including thermal gradients and shrinkage.

For a sandwich wall panel, the temperature differential is considered to be minimal from one wythe to the insulation layer (McCall, 1985), as show on Figure 2-7A. That lead us to the uniform temperature change case discussed in Holmberg & Plem (1965), and the bowing can be computed using equation (2-3).

$$v = +\frac{1}{8} \times \mu t \times \frac{l^2}{r} \times \alpha^2 \left[\left(\frac{2\beta}{\chi l} \right)^2 \times \left(1 - \frac{\cosh \frac{\chi}{\beta} x}{\cosh \frac{\chi l}{2\beta}} \right) - \frac{1}{2} \left(1 - \left(\frac{2x}{l} \right)^2 \right) \right] \quad (2-3)$$

If the temperature varies from the wythe face to the insulation layer, additional moments develop (Figure 2-7B), which could be easily calculated by adding the equations (2-3), (2-4) and (2-5).

$$v = -\frac{l^2}{4} \times \frac{M_o}{EI} \times \left(\frac{\alpha}{\beta} \right)^2 \times \left(\frac{2\beta}{\chi l} \right)^2 \left[\left(\frac{\cosh \frac{\chi}{\beta} x}{\cosh \frac{\chi l}{2\beta}} \right) \right] + \frac{l^2}{4} \times \frac{M_o}{EI} \left[\frac{1}{2} - 2 \left(\frac{x}{l} \right)^2 \right] \quad (2-4)$$

$$v = -\frac{M_o}{EI} \times \left(\frac{l_o}{\beta} \right)^2 \times (\psi_1 \varphi_1 + \psi_3 \varphi_3) \quad (2-5)$$

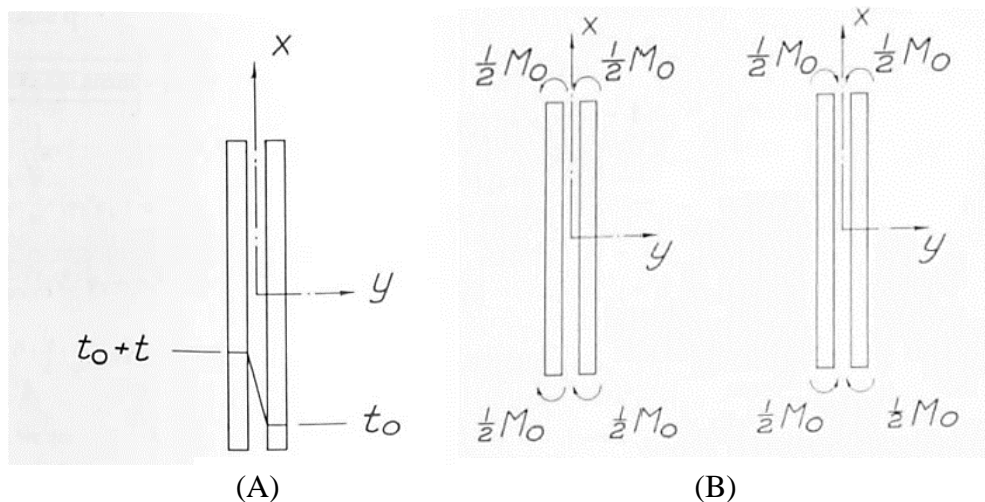


Figure 2-7 Thermal load effect on sandwich panel (Holmberg & Plem, 1965)

Where:

$b =$ Width of the sandwich panel (cm)

$d =$ Thickness of the wythe subjected to the thermal load

$E =$ Modulus of Elasticity (kg/cm²)

$I =$ Fully Composite Moment of Inertia of the panel section(cm⁴)

$i =$ Sum of the moments of Inertia of the two individual wythes (cm⁴)

$$\chi = \sqrt{2kb/EcAc}$$

$k =$ Panel stiffness (kg/cm²/cm)

$l =$ Length of the panel (cm)

$$l_o = \sqrt[4]{\frac{Ei}{2kb}}$$

$$M_o = \frac{1}{2} \frac{\mu \times \Delta t \times EI}{d} \times \beta^2$$

$t =$ Thermal gradient of the whole panel (deg C)

$\Delta t =$ Thermal gradient of a single wythe (deg C)

$x =$ Abscissa (cm), as shown on Figure 2-6

$$\alpha^2 = 2Ar^2/I$$

$$\beta^2 = 1 - \alpha^2$$

$$\lambda = l\sqrt{2}/4l_o$$

$\mu =$ Coefficient of thermal expansion (cm \times C⁻¹ / cm)

$$\xi = x\sqrt{2}/2l_o$$

$\varphi =$ Relative displacement of the wythes (cm)

$$\varphi_1 = \cos(\xi) \cdot \cosh(\xi)$$

$$\varphi_3 = \sin(\xi) \cdot \sinh(\xi)$$

$$\varphi_i^0 = \varphi_i(\lambda)$$

$$\psi = \varphi_1^0 (\varphi_2^0 \times \varphi_4^0) - \varphi_3^0 (\varphi_2^0 \times \varphi_4^0)$$

$$\psi_1 = (\varphi_2^0 - \varphi_4^0) / \psi$$

$$\psi_3 = (\varphi_2^0 + \varphi_4^0) / \psi$$

Leung (1984), tested precast concrete sandwich panels subjected to different thermal gradients, cooling or heating one of the wythes, and compared the results using the equations contained on “Problems and Performance of Precast Concrete Wall Panels” (Leabu, 1960). Although it is unclear the quantity of panels tested, reinforcement in the wythes, connectors used, and spacing, this researcher found the theoretical results to be 25 % higher than the experimental results.

Einea (1992), on “Structural and thermal efficiency of precast concrete sandwich panel systems”, investigated the out-of-plane deflections for a “2-1/2 –3–2-1/2, 30 feet long by 2 feet wide” concrete sandwich panel with truss connector, using finite element analysis (FEA). This researcher determined that equations in Holmberg & Plem (1965), yield similar results to the FEA, however larger deflections all the time.

Ghali, Favre, & Elbadry (2002), did a compilation of different researchs on temperature effects on concrete bridges. They found that the variables which influence thermal gradients the most are: geometry of the cross-section; thermal conductivity, specific heat and density of the material; nature and color of the surface, that is, the absorptivity, emissivity, and convection; orientation of the bridge axis and location; time of the day and season; variation of air temperature and wind speed; and turbidity of the atmosphere. They also pointed that cracked sections exhibits less bending moment than uncracked section, and hence, less deflection due to temperature differentials.

CHAPTER 3

EXPERIMENTAL PROGRAM

3.1 Introduction

The experimental portion of this research was to test a sandwich wall panel with FRP connectors subject to temperature differentials. The goal of this testing was to verify assumptions made by different researchers about the shape of temperature gradients on the panel cross-section, as well as the amount of bowing on the panel due to such temperature change.

3.2 Full-scale test set up

One 16-ft long by 4-ft wide concrete sandwich wall panel was tested to evaluate the effects of temperature differentials on uncracked panels. All connectors were ICON MODEL 23 Carbon Fiber, spaced at 24 inches on center in the long direction and 12 inches on center in the short direction. The insulation used on the panel was XPS, and the reinforcement was ASTM A615 Grade 60 #3 bars spaced 15" each way in both wythes, as shown on Figure 3-1 and Figure 3-2.

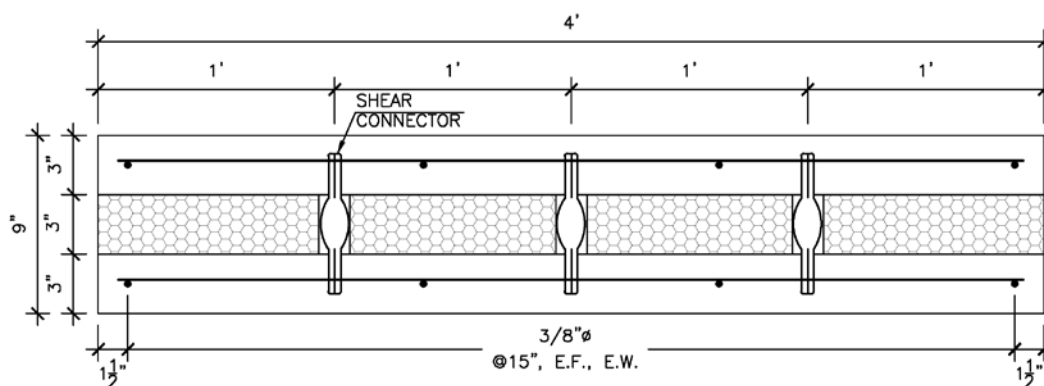


Figure 3-1 Sandwich Panel Cross-Section

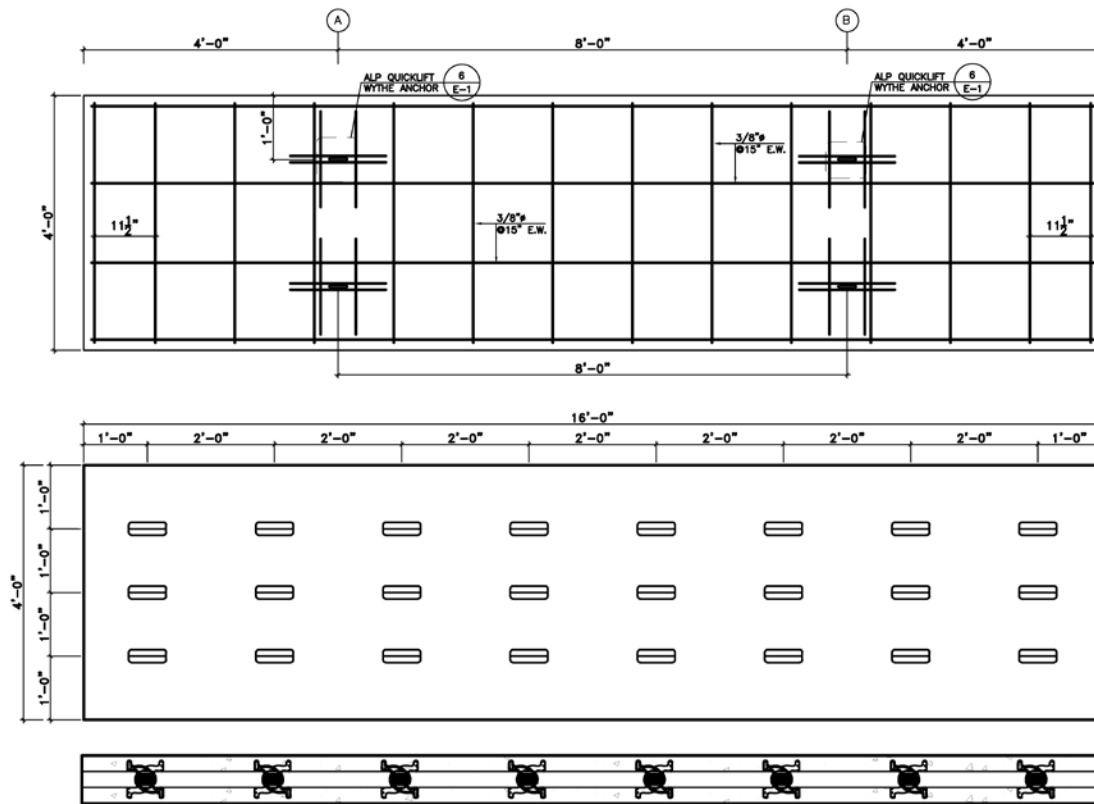


Figure 3-2 Connector and reinforcement layout on sandwich wall panel

The 16-ft long panel was placed on simple supports, with a 15-ft span. An insulated room was built underneath the panel and a 4,000 watts heater was used to increase the temperature in the room to simulate the temperature gradient on the panel. The deflection was recorded at midspan before starting the test with a high accuracy steel ruler by getting the supports and midspan elevations.

The temperature load was tracked with the Campbell Scientific CR1000 datalogger using thermocouple TT-T-20-TWSH-SLE wire. Two thermocouples were embedded in the concrete wythes at one quarter of the total panel length and two at midspan, both at the interface concrete-foam.

Other four thermocouples were also installed, three on the heated face and one on the unheated face, as shown on Figure 3-3. Finally, the concrete compressive strength was determined using the procedure on ASTM C39 for 4 in. by 8 in. concrete cylinders, the tensile strength using ASTM C496, and the modulus of elasticity using ASTM C469.

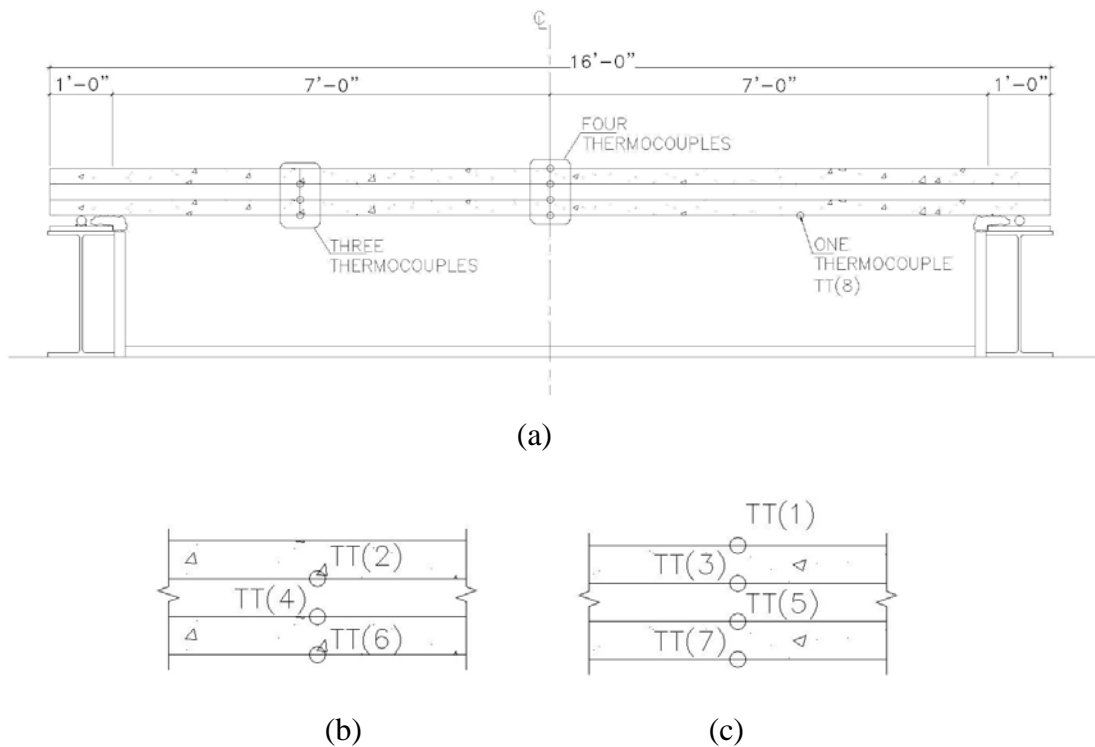


Figure 3-3 Location of thermocouples on sandwich panel – (a) General View, (b) Zoom at one quarter of the panel length (three thermocouples), (c) Zoom at mid-span (four thermocouples)

3.3 Experimental Results

3.3.1 Material Testing Results

The compressive strength test was performed for the concrete associated with the full-scale specimen. The average concrete compressive strength was 5,760 psi, the tensile strength was 645.11 psi and the modulus of elasticity 4,318,000 psi.

The stiffness of the connectors was measured from the slope of the Load vs Deflection curve of two specimens tested, see Figure 3-4. Since the connector shear forces are of opposite signs for thermal and self-weight, the stiffness of the connectors was computed using the average slope of the curve at 0.70 kip, which resulted on a 395 kip/in stiffness.

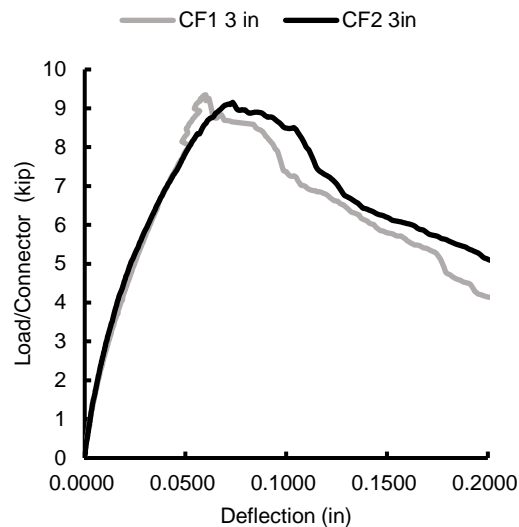


Figure 3-4 Load/Connector vs. Deflection CF 3in Model 23

3.3.2 Full-scale Testing Results

Figure 3-5 shows the temperature variation on different points across the panel. The results can be summarized as follow: (1) the variation in temperature of the unheated wythe was practically zero, which confirms that CFRP connectors do not create thermal bridging; (2) the variation in temperature between two points within the cross section, i.e., surface and interface insulation-concrete was about 8-10 °F (3-5 °C), which can be neglected for design purposes; (3) the temperature gradient on the panel at the end of the testing was approximately 50 °F (30 °C). In addition, the temperature vs. deflection at

mid-span was measured at different arbitrary points in time and the results are shown on Figure 3-6. The trend of the line shows a direct relationship between the temperature differential and the deflection measured, which confirms that the section was still uncracked at the end of the testing, however, the non-linearity of the connector stiffness and the bonding between the foam and the concrete affected the final deflection.

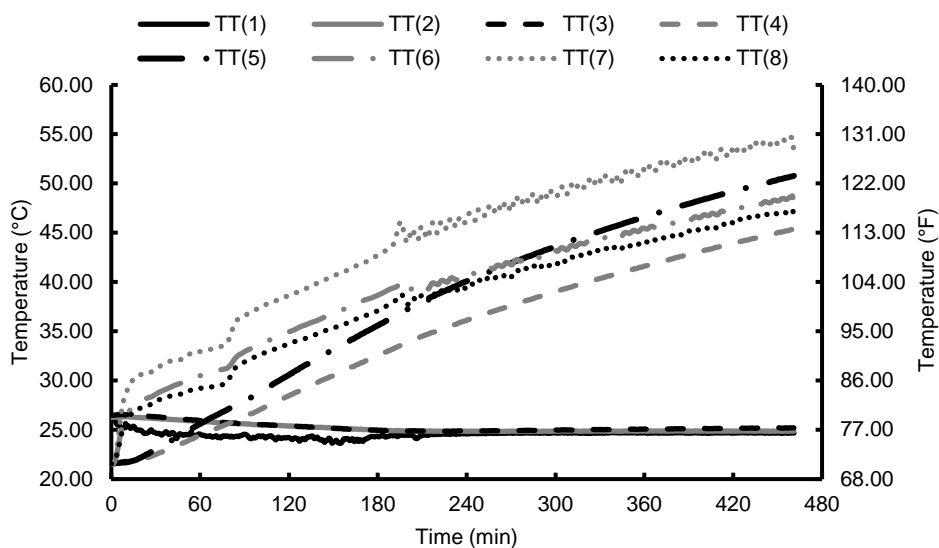


Figure 3-5 Temperature variation on sandwich panel

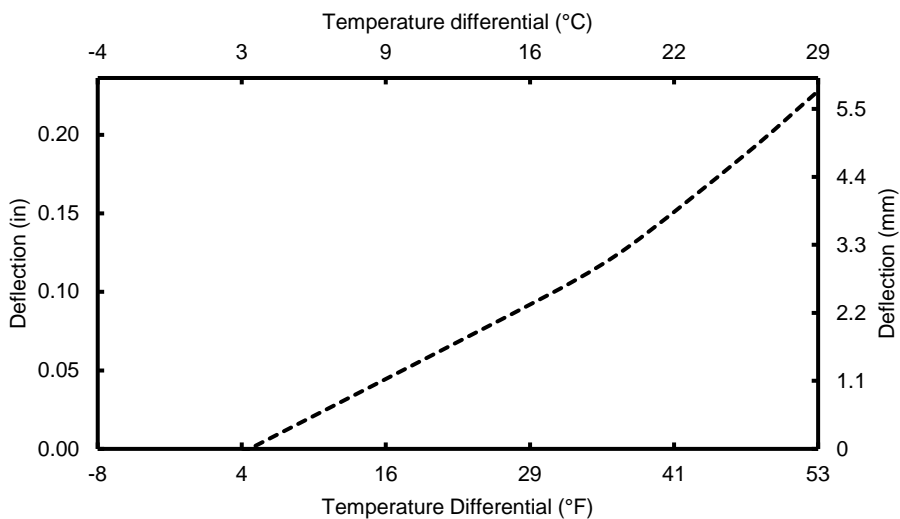


Figure 3-6 Effect of temperature differential on sandwich panel bowing

3.4 Conclusions

A concrete sandwich wall panel was tested at the Utah State University's Systems, Materials, and Structural Health (SMASH) Laboratory. The goal of this testing was to verify assumptions made by different researchers about the behavior of sandwich panels under thermal gradients. The following conclusions can be drawn based on the experimental results:

- The variation in temperature of the unheated wythe is negligible.
- The variation in temperature between two points within the cross section is unimportant.
- There is a linear relationship between bowing and the temperature gradient in the panel.

CHAPTER 4

PARAMETRIC ANALYSIS

4.1 Introduction

Traditional design of Sandwich wall panels generally starts and finish with hand calculations, usually according to linear elastic theory, because of the simplicity these methods represent. However, when the analysis requires information beyond the limits of hand methods, it is pertinent to use the finite element method (FEM). This chapter presents the method and type of elements used, modeling and its validation for mechanical and thermal loads. It also discusses a parametrical analysis of the variables that influence bowing on sandwich wall panels.

4.2 Finite Element Analysis

As mentioned before, the finite element method gives the advantage of capturing the behavior of the panel's components beyond hand methods capacity, that is, the elastic connectors' slip, shear and axial forces can be tracked, as well as the concrete wythe's stresses and deformations.

4.2.1 Beam-Spring Model

For a long time, the truss model and beam-spring model have been the main model used in the finite element analysis of SWPs, tunnel pre-reinforcing system, etc., even though commercial software capable of performing the analysis of more sophisticated models is available, which can capture some extra information of the model in a modest time. The beam-spring model assumes that the panel stresses and

deformations, connector forces and slip variations are negligible in the short direction of the panel. The advantages of having a simple model as the beam-spring model is that it allows to create a model faster, more user friendly and simpler.

4.2.2 Shell–Spring Model

Due to the simplicity of the beam-spring or truss model, the shell spring model is not used often in structural engineering, however, when large complex problems require observing the variation of parameters in three dimensions, the shell-spring model suits perfectly. Examples of these applications are the shield tunnel segmental lining analysis (Zhu, Huang, & Liang, 2006), and the optimization of radial tire contour (Unnithan, KrishnaKumar, & Prasad, 2003). Since the goal of this research was to investigate all the possible parameters influencing the behavior of SWPs subject to temperature variations, the Shell–Spring model was chosen.

4.3 Validation of the Shell-Spring Model

Since the scope of this thesis was to test panels subject to temperature differentials, a full-scale testing to study the panel subject to mechanical loads was not performed. The validation of the model for this type of loading was based on the prediction of the deflection of panel “HK-2” shown on Al-Rubaye, Sorensen, & Maguire (2017). For this panel results the shell-spring model underestimate the deflection by 4.16% (see Figure 4-1), which is an acceptable difference for a concrete member (Nowak & Collins, 2012).

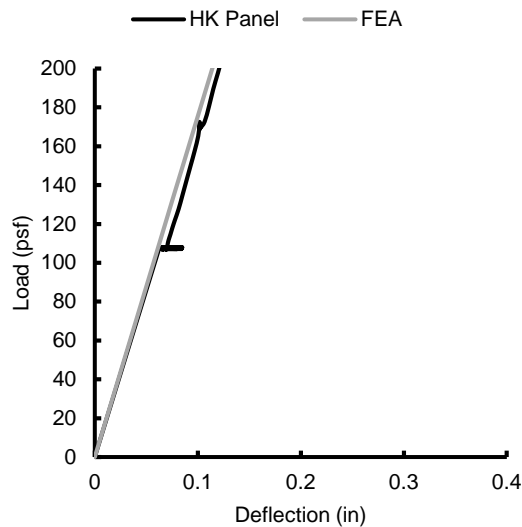


Figure 4-1 Load versus deflection for "HK-2" Panel

The comparison between the experimental results for thermal loads is shown on Figure 4-2. In this case, the FEA model underestimate the deflection by approximately 15%, mainly because of the panel size and the precision of the instrumentation. Further testing might be adequate to calibrate the model.

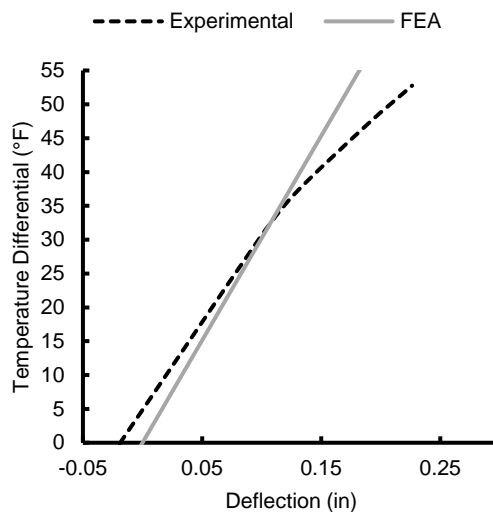


Figure 4-2 Temperature differential versus deflection for full-scale panel test and FEA

4.4 Parametric Study

All studied models were analyzed using a three-dimensional finite element proprietary software, considering the panels to be a simply supported shell connected to another one by spring elements. A uniform temperature load was applied to the unsupported shell while leaving the shell on supports free to move. The parameters studied were the following: stiffness of the panel, compressive strength of concrete, length of the panels¹, distance between centroid of the wythes, temperature load, and coefficient of thermal expansion.

4.4.1 Effect of Panel Stiffness

The stiffness of a sandwich panel is one of the most important variables in the design of SWPs, it can be defined as the sum of the connector stiffness divided by the area of the panel, and hence, either a variation in stiffness of the connectors or the separation of them affects the overall panel stiffness. If the panel stiffness vary for a set of panels, the following observations can be made: bowing, the maximum connector rotation, axial and shear force, and the stresses on the wythes increase as the panel stiffness increase, as shown on Figure 4-3 to Figure 4-6. It was also found that for all panel lengths, the maximum connector shear and axial force was approximately the same provided the same panel stiffness was provided. The maximum connector slip, however, decreases as the panel stiffness increases (see Figure 4-3).

¹ All panel are simple span with a length equal to the panel length minus two (2) feet.

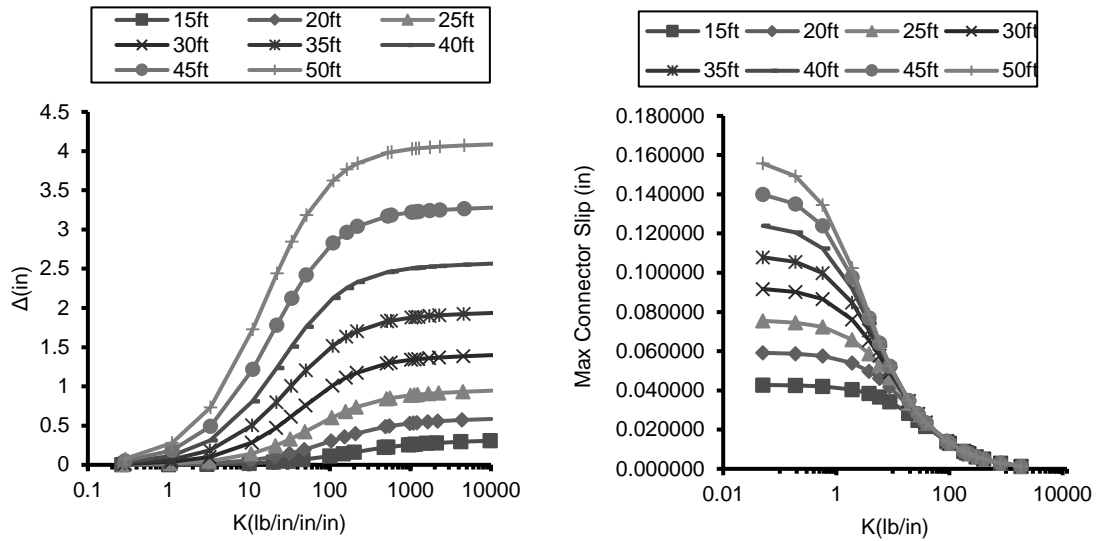


Figure 4-3 Effect of Panel Stiffness on Out-of-Plane Deflection (left) and Connector Rotation (right) of a 3-2-3 Panel

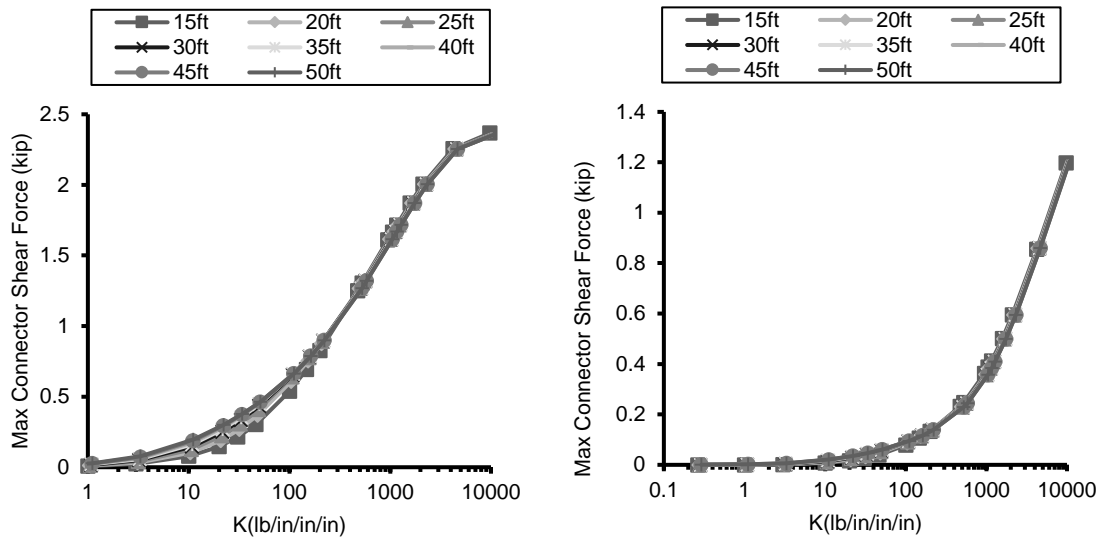


Figure 4-4 Effect of Panel Stiffness on maximum Connector Shear Force (left) and Axial Force (right) of a 3-2-3 Panel

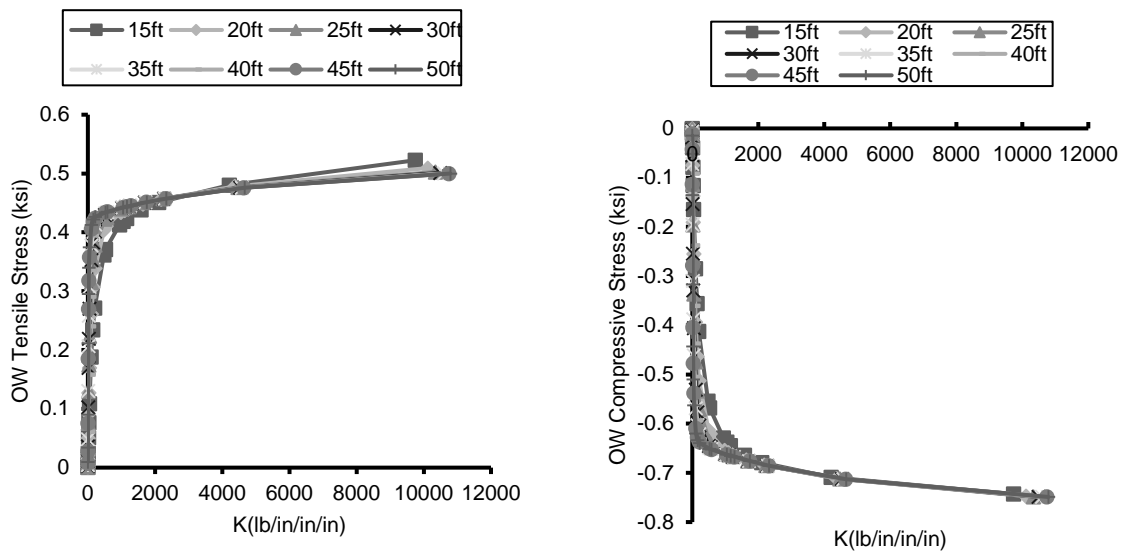


Figure 4-5 Effect of Panel Stiffness on Heated Wythe (OW) Stress, Tensile (left) and Compressive (right) of a 3-2-3 Panel

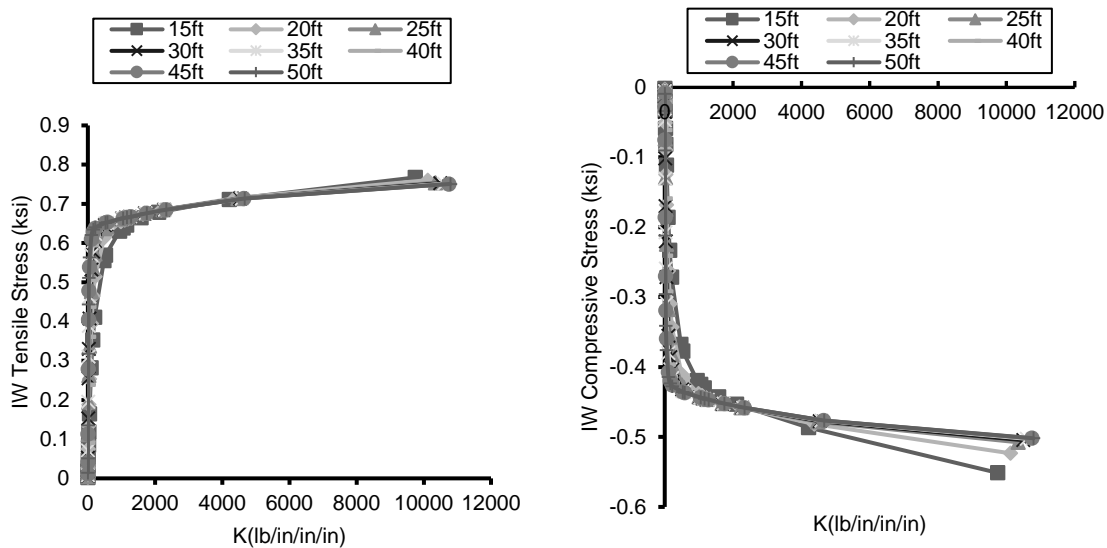


Figure 4-6 Effect of Panel Stiffness on Unheated Wythe (IW) Stress, Tensile (left) and Compressive (right) of a 3-2-3 Panel

4.4.2 Effect of Panel Length

The second variable that most influences the behavior of SWPs is the length of the panel. For a given connector stiffness and thermal gradient, as the panel length increases, bowing, maximum connector rotation, slip, shear and axial forces increase. However, the increase in force, displacement and rotations associated with the connectors is more pronounced on low stiffness panels, and panels of different wythe's sizes. Figure 4-7 to Figure 4-11 show the variation in the previously mentioned variables for 3-2-3 panels subject to a 100 F temperature differential, with overall stiffness of 100-110 kip/in³. Although the variation on shear and axial force in the connector was about 25%, the value itself is not significant, and the variation can be assumed constant.

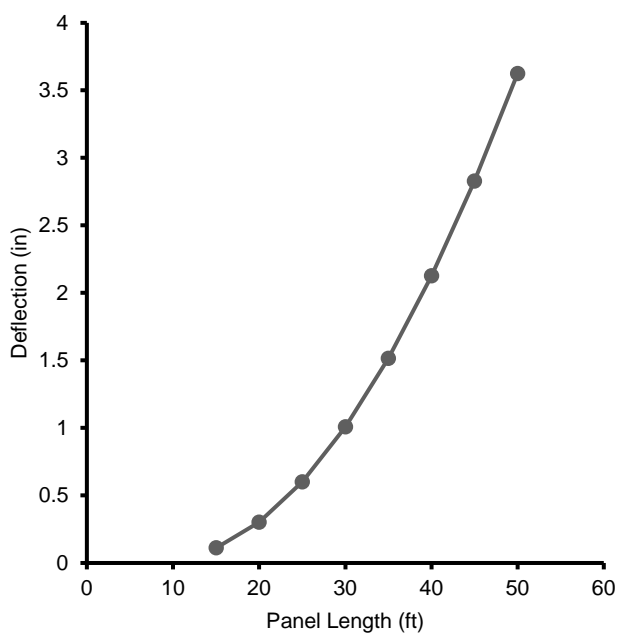


Figure 4-7 Effect of Panel Length on Deflection

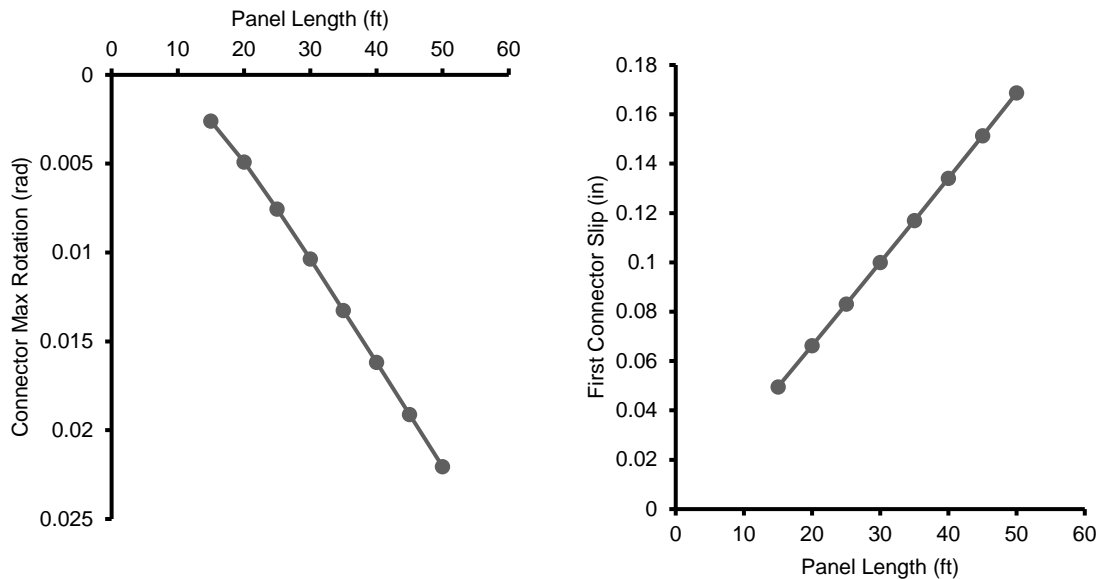


Figure 4-8 Effect of Panel Length on Connector Maximum Rotation (left), and Maximum Slip (right)

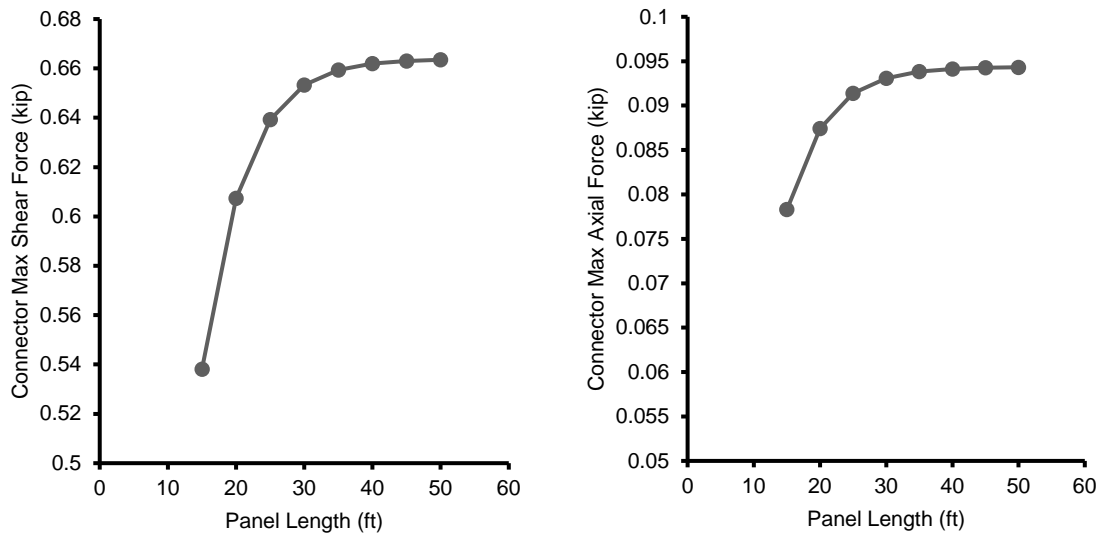


Figure 4-9 Effect of Panel Length on maximum Connector Shear Force (left) and Axial Force (right) of a 3-2-3 Panel

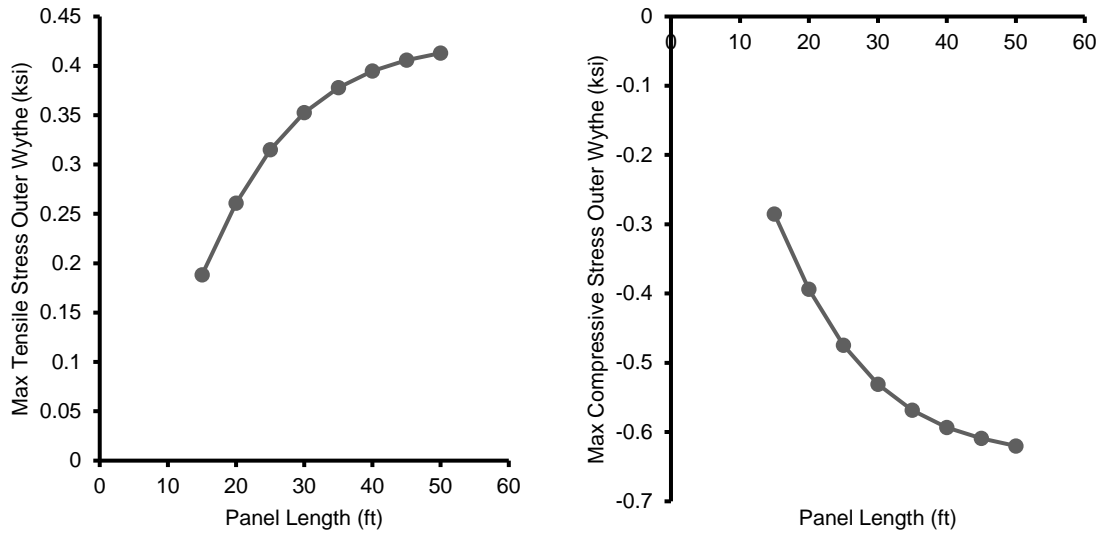


Figure 4-10 Effect of Panel Length on Heated (Outer) Wythe Stress, Tensile (left) and Compressive (right) of a 3-2-3 Panel

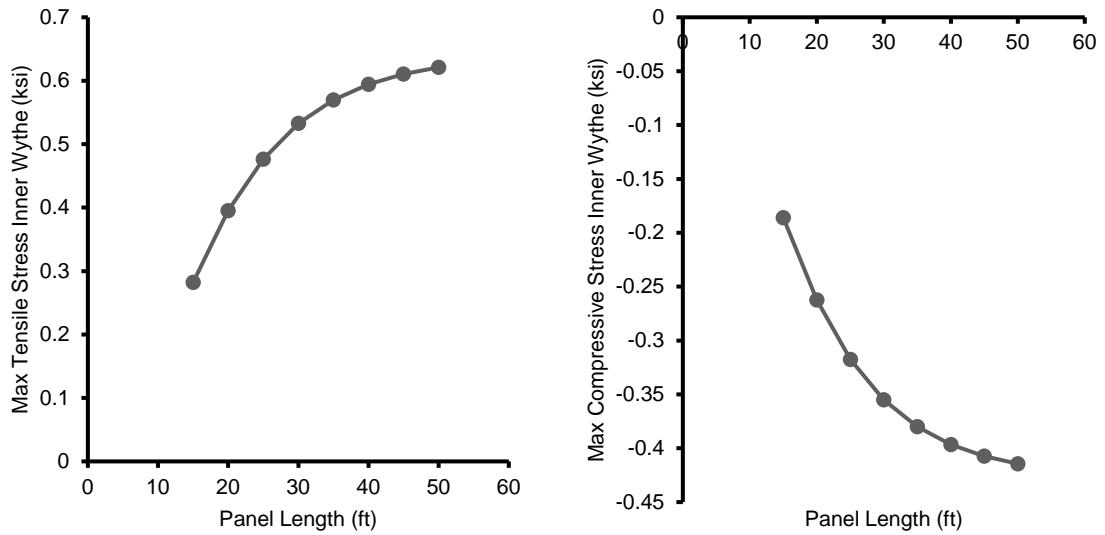


Figure 4-11 Effect of Panel Length on Unheated (inner) Wythe Stress, Tensile (left) and Compressive (right) of a 3-2-3 Panel

4.4.3 Effect of distance between wythes centroid

The distance between wythes' centroids "d" can vary either by either increasing the wythe's thickness or increasing the insulation size. In tilt-up SWPs it is common to have panels of different wythe sizes and, if a stiffer panel is needed the designer opt to increase the inner wythe thickness. In other cases, especially in partially or fully composite panels, the engineer will increase both concrete layer thicknesses the same amount to satisfy strength and serviceability requirements. Although both practices tend to reduce bowing, concrete stresses, and connector forces and deformations variations are unknown. Figure 4-12 shows the bowing for the following panels: 3-3-4, 3-3-6, 3-3-8, 3-3-8, 3-3-10 and 3-3-12 panels, on the left; 4-3-4, 6-3-6, 8-3-8, 10-3-10 and 12-3-12, on the right, for overall stiffness of 500-600 kip/in³. In both cases as the distance "d" increases, bowing decreases drastically, being the non-uniform variation the most favorable.

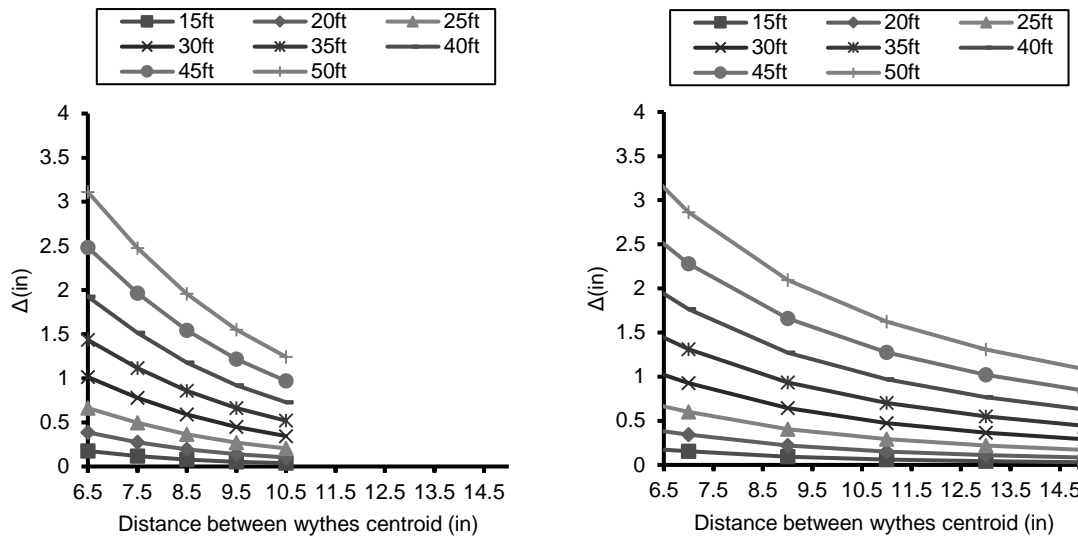


Figure 4-12 Effect of distance between wythes centroid on thermal bowing, non-uniform wythe's variation (left) and uniform wythe's variation (right)

The benefit of increasing the thickness of the panel is not always favorable, in the case of tensile stress on an uncracked section, it decreases for the warmer wythe and increase or decrease for the colder wythe depending on the length of the panel and whether the wythes vary with respect of each other, see Figure 4-13 and Figure 4-14.

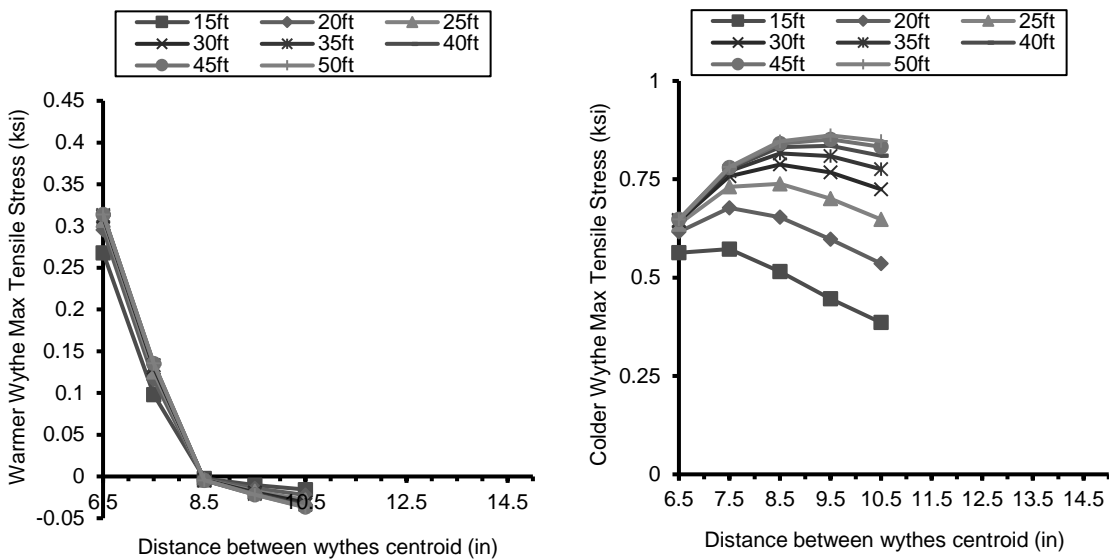


Figure 4-13 Effect of Distance "d" on tensile stress of panels with unequal wythes.

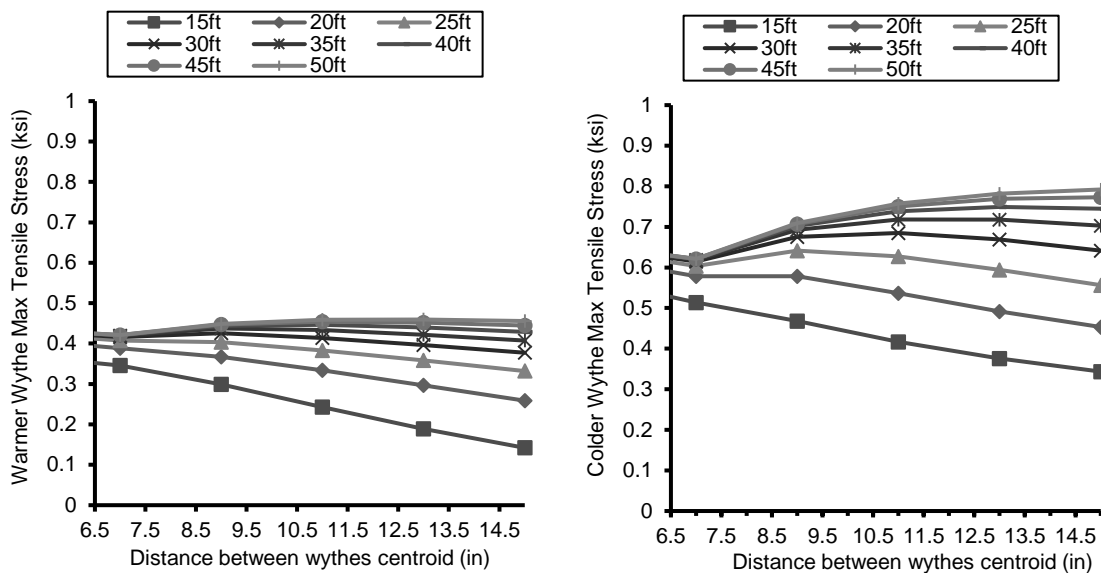


Figure 4-14 Effect of Distance "d" on tensile stress of panels with equal wythes.

In the case of connector forces, the shear force increases by either thickening one concrete layer or both at the same time, however, the axial force decreases for unequal wythes and increases for wythes of the same size.

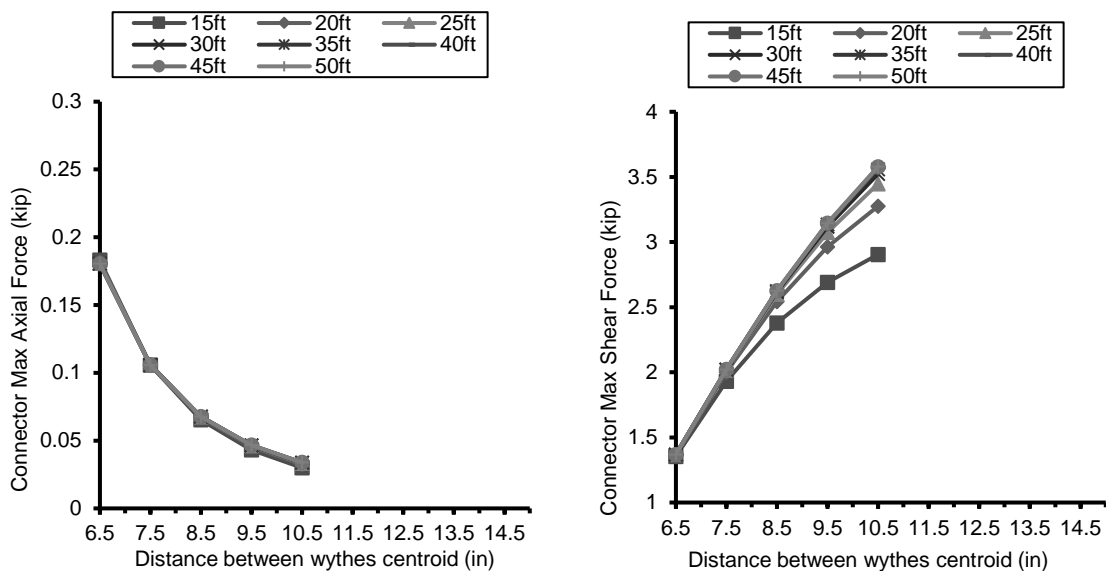


Figure 4-15 Effect of Distance "d" on connector forces of panels with unequal wythes

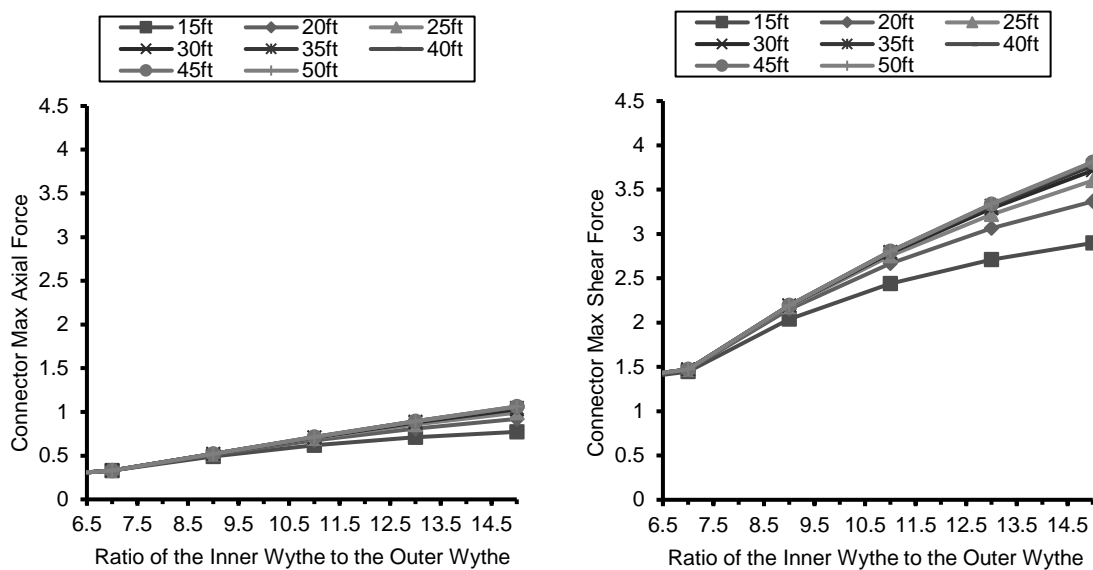


Figure 4-16 Effect of distance "d" on connector forces of panels with equal wythes

4.4.4 Effect of temperature

Unlike most of the variables studied so far, temperature gradients have a linear relation with bowing, end connector slip, tensile stress and connector forcings, as shown on Figure 4-17 to Figure 4-19.

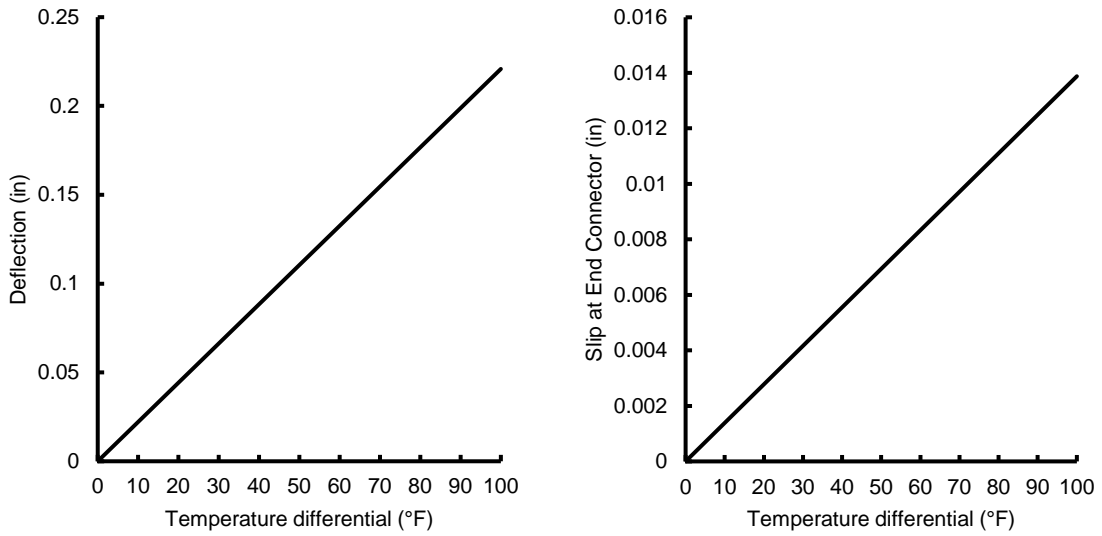


Figure 4-17 Effect of temperature on deflection (left) and slip (right) of a 15 ft. long by 8 ft. wide panel with a 323 configuration

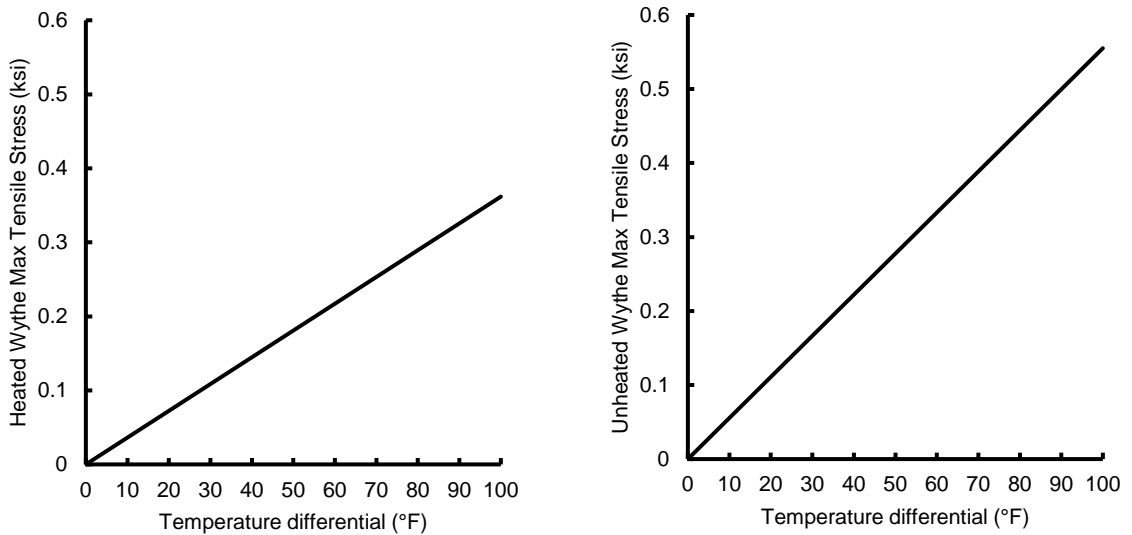


Figure 4-18 Effect of temperature on tensile stress of heated (left) and unheated (right) wythes of a 15 ft. long by 8 ft. wide panel with a 323 configuration

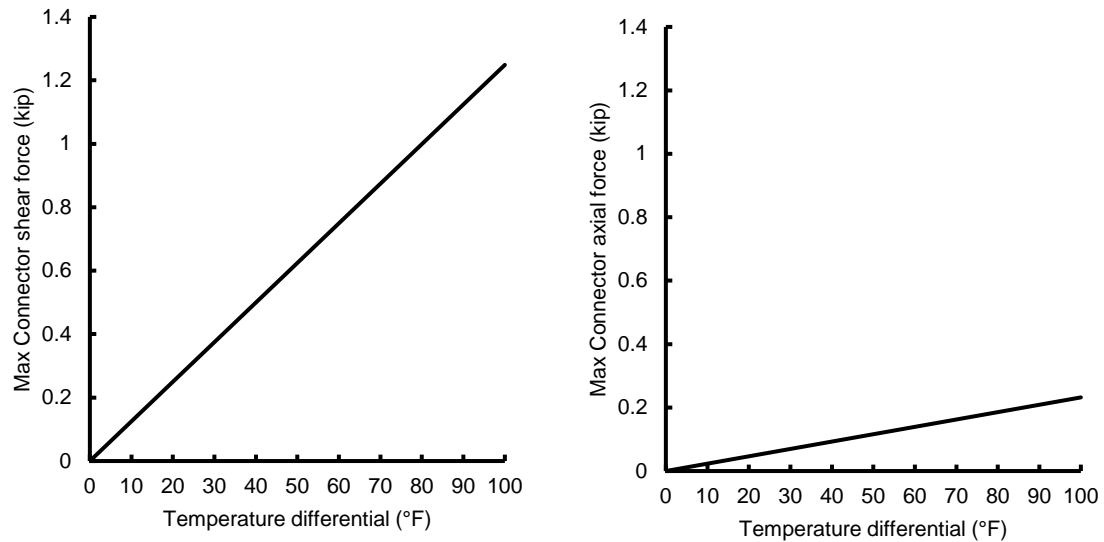


Figure 4-19 Effect of temperature on connector shear (left) and axial (right) forces of a 15 ft. long by 8 ft. wide panel with a 323 configuration

4.4.5 Effect of concrete properties

Concrete properties have different effects on bowing, that is, as the coefficient of thermal expansion increases bowing increases linearly, as shown on Figure 4-20. In other words, a 20% increase on the coefficient of thermal expansion increases bowing 20%. Also, the modulus of elasticity (E_c) plays an important role on bowing, when it increases, the deflection tends to be more uniform and the connector shear maximum force increases, as well as the panel internal forces and hence, the maximum tensile stress. It is also worth to mention, that an increase in compressive strength of concrete helps to prevent cracking of concrete sandwich wall panels, but the setback caused by the stress increase could also result in cracking and should be considered during the design process.

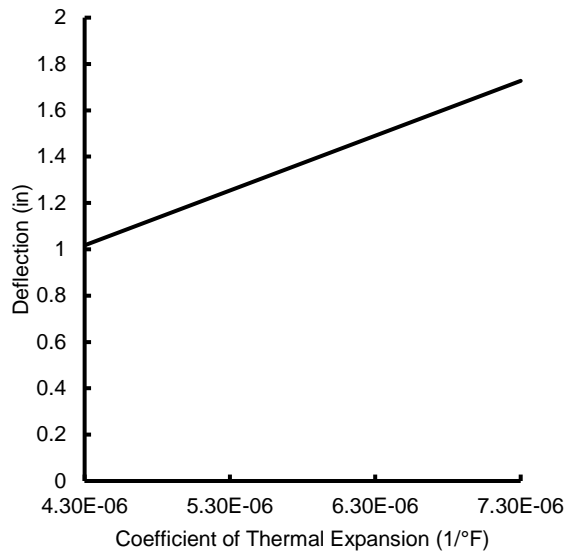


Figure 4-20 Effect of coefficient of thermal expansion on bowing

Figure 4-21 shows the difference in tensile stress on a 3-2-3, 15-ft long by 8ft wide panel with 400 kip/in connectors spaced at 12 inches on center, each way and a 100°F thermal gradient. The span length for this wall was 15-ft and the concrete compressive strength 4ksi and 8-ksi. As the plot shows, doubling the strength is not exactly beneficial for the sandwich panel, and hence, should be considered in the design process. The limit set on the tensile stress is $7.5 \sqrt{f'_c}$, as recommended by the ACI 318-14. The connector shear force is also affected by the change on compressive strength of concrete, as shown on Figure 4-22.

4.5 Holmberg and Plem Equation, FEA and PCI Equation Comparison

If we take equation (2-3) and evaluate it at mid-span, for sandwich panels of unequal size wythes, it takes the following form:

$$v = +\frac{1}{4} \times \mu t \times \frac{l^2}{(r_1 + r_2)} \times \alpha^2 \left[\left(\frac{2\beta}{\chi l} \right)^2 \times \left(1 - \operatorname{sech} \frac{\chi l}{2\beta} \right) - \frac{1}{2} \right] \quad (4-1)$$

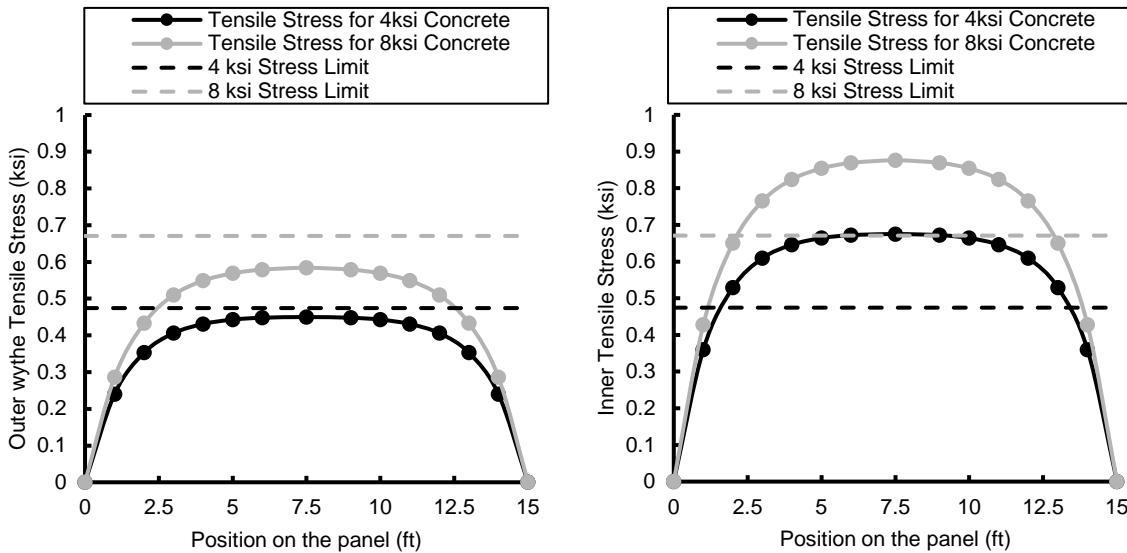


Figure 4-21 Effect of change in compressive strength on outer wythe tensile stress (left) and inner wythe tensile stress (right)

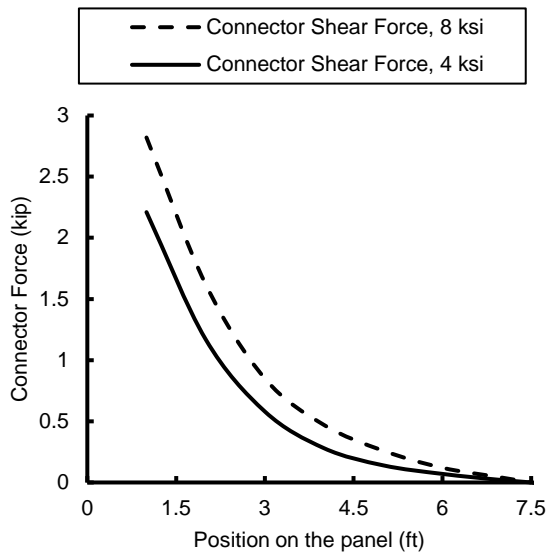


Figure 4-22 Effect of change in compressive strength on connector shear force

Also, the term χ , takes the form:

$$\chi = \sqrt{\frac{k(t_1 + t_2)}{t_1 t_2 E c}} \quad (4-2)$$

Where t_1 and t_2 are the thickness of the wythes, and r_1 and r_2 are the distance between the first and second wythe cross-section center of gravity (c.g.) and the centroid of the whole section, respectively.

Equations (2-3) and (4-1) can be simplified² to more practical terms and expressed as a function of the percentage of composite action as follow:

$$\Delta_{midspan} = \frac{1}{8} \times c \times \Delta T \times \frac{l^2}{d} \times \frac{I_{FC} - I_{NC}}{I_{FC}} \left[1 - \operatorname{sech} \frac{\chi l}{2\beta} \right] \quad (4-3)$$

Or:

$$\Delta_{midspan} = \frac{1}{8} \times c \times \Delta T \times \frac{l^2}{d} \times \frac{I_{FC} - I_{NC}}{I_{FC}} \%PCA \quad (4-4)$$

Figure 4-23 shows a comparison of equations (2-1), (4-1) and the FEA results for a 3-3-8, 30 ft. long by 8ft width panel with a span of 28 ft, subjected to a thermal gradient of 100 °F. For the equation found on PCI handbook, the deflection tends to be at least 25% larger than either equation (4-1) or the FEA results.

² This simplification overestimates the deflection.

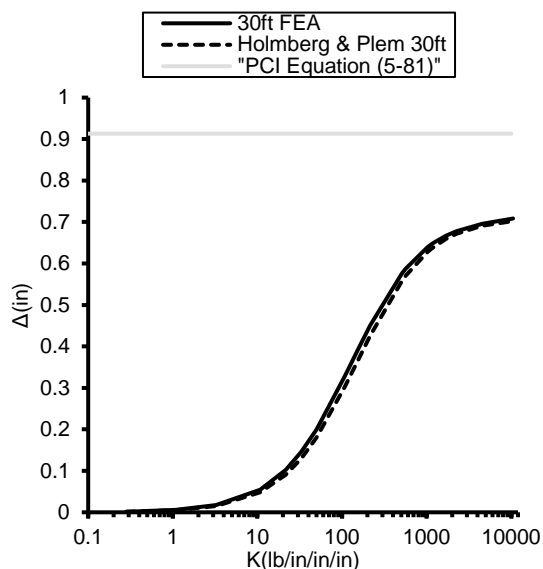


Figure 4-23 Comparison of different bowing computation equations and FEA

Table 4-3 and Table 4-4 show a comparison of equations (2-3), (4-1) and the FEA for a set of panels. For short panels, 15 ft. long, the difference between these two methods is as high as 34% for 3-2-3 panels and 21% for 3-3-8 panels, which decreases as stiffness and/or length increases. For example, the 3-3-8 panel average difference for a 50 ft. is 2.86% and 1.56% for panels with 400 kip/in. connectors, spaced 12 in. on center.

Table 4-1 Difference between FEA and equation (2-3) for a 323 panel

Kconn	0.19	3.80	5.80	8.80	19.00	28.00	38.00	100.00	200.00	300.00	400.00
15 ft	0.0007	0.0080	0.0107	0.0139	0.0193	0.0208	0.0210	0.0158	0.0107	0.0088	0.0081
20 ft	0.0018	0.0184	0.0233	0.0278	0.0318	0.0305	0.0282	0.0169	0.0107	0.0092	0.0090
25 ft	0.0035	0.0310	0.0367	0.0402	0.0384	0.0336	0.0288	0.0140	0.0077	0.0066	0.0067
30 ft	0.0060	0.0460	0.0511	0.0524	0.0442	0.0368	0.0306	0.0146	0.0086	0.0078	0.0081
35 ft	0.0093	0.0594	0.0620	0.0596	0.0448	0.0355	0.0284	0.0119	0.0063	0.0056	0.0060
40 ft	0.0137	0.0733	0.0728	0.0667	0.0471	0.0367	0.0293	0.0130	0.0077	0.0071	0.0076
45 ft	0.0189	0.0834	0.0789	0.0691	0.0454	0.0342	0.0266	0.0107	0.0056	0.0052	0.0057
50 ft	0.0252	0.0939	0.0857	0.0729	0.0465	0.0351	0.0275	0.0120	0.0072	0.0068	0.0074

Table 4-2 Difference between FEA and equation (4-1) for a 3-3-8 panel

Kconn	0.19	3.80	5.80	8.80	19.00	28.00	38.00	100.00	200.00	300.00	400.00
15 ft	0.0001	0.0010	0.0017	0.0026	0.0050	0.0066	0.0079	0.0106	0.0098	0.0084	0.0074
20 ft	0.0000	0.0033	0.0049	0.0069	0.0115	0.0137	0.0150	0.0150	0.0114	0.0090	0.0075
25 ft	0.0001	0.0068	0.0095	0.0126	0.0183	0.0200	0.0204	0.0159	0.0103	0.0075	0.0059
30 ft	0.0004	0.0117	0.0158	0.0199	0.0256	0.0262	0.0253	0.0171	0.0106	0.0078	0.0062
35 ft	0.0010	0.0176	0.0226	0.0271	0.0310	0.0298	0.0274	0.0162	0.0092	0.0064	0.0049
40 ft	0.0017	0.0247	0.0305	0.0350	0.0363	0.0333	0.0297	0.0167	0.0096	0.0069	0.0055
45 ft	0.0026	0.0319	0.0378	0.0414	0.0392	0.0344	0.0297	0.0154	0.0084	0.0057	0.0044
50 ft	0.0038	0.0400	0.0457	0.0480	0.0424	0.0362	0.0308	0.0158	0.0089	0.0064	0.0051

Table 4-3 Percentage differential between FEA and equation (2-3) for a 323 panel

Kconn	0.19	3.80	5.80	8.80	19.00	28.00	38.00	100.00	200.00	300.00	400.00
15 ft.	21.89%	19.06%	20.36%	20.97%	20.56%	19.64%	18.58%	13.63%	9.44%	7.22%	5.92%
20 ft.	-0.40%	16.94%	16.93%	16.52%	14.77%	13.42%	12.17%	7.69%	4.83%	3.55%	2.85%
25 ft.	5.18%	13.75%	13.28%	12.53%	10.42%	9.05%	7.90%	4.36%	2.47%	1.71%	1.32%
30 ft.	8.02%	11.49%	10.84%	9.97%	7.83%	6.59%	5.60%	2.92%	1.65%	1.16%	0.92%
35 ft.	8.70%	9.48%	8.75%	7.84%	5.81%	4.73%	3.92%	1.88%	1.00%	0.68%	0.52%
40 ft.	8.72%	8.06%	7.31%	6.41%	4.54%	3.63%	2.97%	1.42%	0.78%	0.55%	0.43%
45 ft.	8.22%	6.80%	6.03%	5.17%	3.50%	2.73%	2.20%	1.00%	0.52%	0.35%	0.27%
50 ft.	7.72%	5.87%	5.12%	4.31%	2.83%	2.19%	1.76%	0.81%	0.44%	0.31%	0.25%

Table 4-4 Percentage differential between FEA and equation (4-1) for a 3-3-8 panel

Kconn	0.19	3.80	5.80	8.80	19.00	28.00	38.00	100.00	200.00	300.00	400.00
15 ft.	34.07%	24.84%	23.31%	21.54%	17.43%	14.98%	12.95%	6.96%	4.14%	3.23%	2.91%
20 ft.	26.52%	17.74%	16.15%	14.35%	10.54%	8.57%	7.10%	3.43%	2.02%	1.68%	1.62%
25 ft.	20.65%	12.77%	11.23%	9.57%	6.41%	4.94%	3.93%	1.65%	0.87%	0.72%	0.73%
30 ft.	16.88%	9.77%	8.36%	6.91%	4.39%	3.32%	2.61%	1.12%	0.64%	0.57%	0.59%
35 ft.	14.01%	7.44%	6.18%	4.95%	2.96%	2.17%	1.67%	0.65%	0.34%	0.30%	0.32%
40 ft.	12.01%	5.93%	4.83%	3.79%	2.22%	1.63%	1.26%	0.53%	0.31%	0.28%	0.30%
45 ft.	10.31%	4.68%	3.72%	2.85%	1.60%	1.15%	0.88%	0.34%	0.17%	0.16%	0.18%
50 ft.	9.06%	3.85%	3.01%	2.29%	1.28%	0.93%	0.72%	0.30%	0.18%	0.17%	0.18%

4.6 Estimation of the percentage of composite action (PCA)

The current methods for computing the PCA on concrete sandwich panels are two. The first one is based on the cracking deflection observed during the testing of a sandwich panel. For this deflection, we find the theoretical moment of inertia that corresponds to the testing load case. The result is compared with the theoretical fully composite and non-composite moment of inertia, and the resulting value is the percentage of composite action, see equation (4-5).

$$\kappa = \frac{I_{exp} - I_{NC}}{I_{FC} - I_{NC}} \times 100 \quad (4-5)$$

The second one uses a similar approach; however, it takes the linear slope of the load deflection curve of a sandwich panel and compares it to the fully composite and non-composite load vs deflection curves. These slopes are analyzed using the following equation:

$$\kappa = \frac{Slope_{exp} - Slope_{NC}}{Slope_{FC} - Slope_{NC}} \times 100 \quad (4-6)$$

If we take the full-scale testing on section 3.2 and compute the percentage of composite action with the previously mentioned method, it results on a 94.27% of composite action. On the other hand, if we take the variable portion of equation (4-3), it results on a 97.60% of composite action. The main reason for this difference is that the degree of shear transfer between the two wythes changes nonlinearly (see Figure 4-23), which results in an overestimation of the real result by the equation (4-6). The following

equation, taken from equation (4-3), provides an accurate method for computing the degree of elastic composite action³:

$$\kappa = \left(1 - \operatorname{sech} \frac{\chi l}{2\beta}\right) \quad (4-7)$$

4.7 Conclusions

A parametric analysis was performed in this section. This allowed us to identify the variables that affect thermal bowing within the scope of this research, and draw the following conclusions:

- The maximum connector rotation, axial and shear force, and the stresses on the wythes increase as the panel stiffness increase.
- For a given panel stiffness, the maximum connector shear and axial force is the same, regardless of the panel length.
- The maximum connector slip decreases as the panel stiffness increases.
- Bowing and the span length have a quadratic relationship.
- The distance between wythe's centroids and bowing have an inverse relation.
- The coefficient of thermal expansion and bowing have a linear relationship.

³ This method is discussed more in depth in the next chapter.

- The variation on compressive strength does not affect bowing significantly, however, an increase in compressive strength can avoid cracking.
- PCI handbook equation 5-81 yields higher deflections values than either FEA or Holmberg & Plem (1965) equation.
- A equation for computing the percentage of composite action was proposed and compared with a current method.

CHAPTER 5

SERVICIABILITY ANALYSIS

5.1 Introduction

As discussed in chapter 4, deformations due to thermal bowing can be significantly large when panels are subject to temperature differentials greater than 60 °F, and consequently, the out of plane $P-\delta$ contribution must be analyzed along other load combinations. This chapter shows the steps necessary to perform such analysis and the assumptions associated with it.

5.2 Sandwich Wall Panels with Out-of-Plane Bending

The in-plane behavior of concrete walls is normally controlled by the $P-\Delta$ contribution, while the $P-\delta$ contribution is often ignored for simplicity. On the other hand, the out-of-plane behavior is controlled by a combination of both effects and ignoring the $P-\delta$ effect can result in out-of-plane buckling of the wall (Powell, 2010). The loads causing bending can be due to earthquakes, wind or temperature changes, which are amplified by the axial stress on the wall and deflect the panel beyond a basic mechanics analysis calculation. The case studied in this section corresponds to sandwich wall panels subject to thermal bowing, dead load of simple span walls with bending deformations within its length and no joint translation, hence, considered non-sway, as shown on Figure 5-1. Since the thermal gradient and the dead load moment, generated by the eccentricity of the roof reaction on the wall, have different moment diagrams a detailed analysis should be performed to get the point of maximum amplifications.

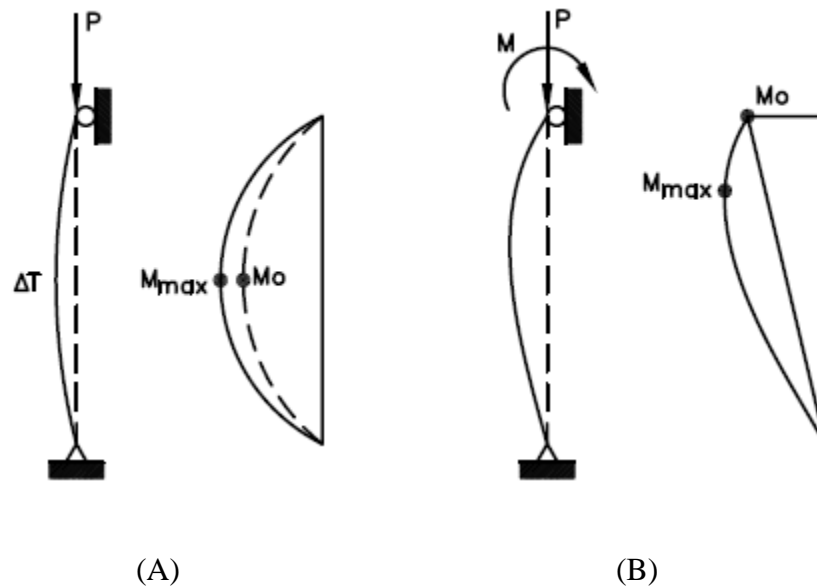


Figure 5-1 Example of moment amplification

5.3 P- δ Analysis of Uncracked SWPs

ACI 318-14 code in section 6.6 incorporates the provisions to assess the slenderness effects on sway and non-sway columns and walls. In addition, the PCI handbook in section 5.9.3 provides additional recommendations regarding the analysis, reasons and calculations to take into account these secondary effects on precast concrete columns and walls. The following procedure consider such steps incorporating thermal bowing, stiffness of the connectors and the ACI 318-14 guidance in section R6.2.6.

1. Perform a load analysis.
2. Pick a trial sandwich wall panel section and material properties.
3. Select a preliminary steel area.
4. Perform a shear flow analysis to find the total number of connectors.
5. Compute section properties.

6. Calculate the effective stiffness of the panel for thermal bowing and gravity loads, this is at least $0.85EcIg$ for thermal bowing.
7. Find the deflection at the critical point⁴ due to temperature using equation (2-3).
8. Compute the deflection at the critical point due to the axial load on the panel.
9. Add thermal bowing, dead load deflection and initial panel bowing together and repeat step 8 to find the total deflection at the critical point due to axial load on the panel until it converges.
10. Determine whether the section remains uncracked for the applied loads. If not, resize panel or change the shear connector type and/or distribution.

5.4 Computation of Forces and deformations on Sandwich Wall panels

The P-Delta analysis of sandwich wall panels requires the knowledge of the moments and axial force on the panel, along with the deformations. This section presents the basis of a method for finding those forces and deformations and provides guidance on how to use the equations. If we take the nailed sandwich beam theory from Granholm (1949), and apply it to sandwich wall panels of different wythe thickness and the same modulus of elasticity, we have the following:

$$\varphi'' - \chi^2 \varphi = (r_1 + r_2)v''' \quad (5-1)$$

⁴ The critical point is usually taken at mid-height of the panel.

and,

$$v'' - \frac{\alpha^2}{r_1 + r_2} \varphi' = -\frac{M_x}{EI} \quad (5-2)$$

By applying a thermal gradient between the two concrete wythes, one with a constant temperature increment across all dimensions of the panel and the other one with no temperature increase, the equation (5-2) takes the following form:

$$v'' - \frac{\alpha^2}{r_1 + r_2} \varphi' = -\frac{\alpha^2}{r_1 + r_2} c \times \Delta T \quad (5-3)$$

After solving the differential equations (5-1) and (5-3), we get the following:

Slip:
$$\varphi = -c \times \Delta T \frac{\beta}{\chi} \left(\frac{\sinh \frac{\chi}{\beta} x}{\cosh \frac{\chi l}{2\beta}} \right) \quad (5-4)$$

Connector Shear force:
$$F_{shear} = \varphi k_{conn} \quad (5-5)$$

Moment on first wythe:
$$M_1 = -\frac{\alpha^2}{r_1 + r_2} c \times \Delta T \times E_c \times i_1 \left(1 - \frac{\cosh \frac{\chi}{\beta} x}{\cosh \frac{\chi l}{2\beta}} \right) \quad (5-6)$$

Moment on second wythe:
$$M_2 = -\frac{\alpha^2}{r_1 + r_2} c \times \Delta T \times E_c \times i_2 \left(1 - \frac{\cosh \frac{\chi}{\beta} x}{\cosh \frac{\chi l}{2\beta}} \right) \quad (5-7)$$

Axial force on either wythe:
$$N = -\frac{\alpha^2}{(r_1 + r_2)^2} c \times \Delta T \times E_c \times I_{NC} \left(1 - \frac{\cosh \frac{\chi}{\beta} x}{\cosh \frac{\chi l}{2\beta}} \right) \quad (5-8)$$

$$\text{Deflection: } v = -\frac{\alpha^2}{(r_1 + r_2)^2} c \times \Delta T \times \left[\left(\frac{\beta}{\chi}\right)^2 \left(1 - \frac{\cosh \frac{\chi}{\beta} x}{\cosh \frac{\chi l}{2\beta}}\right) + \left(\frac{x^2}{2} - \frac{l^2}{2}\right) \right] \quad (5-9)$$

These equations provide an exact solution for the panel forces and deformations, provided the user input the correct stiffness values. Since the panel stiffness varies depending on several factors, a simplification on how to compute the stiffness of the panel is necessary. For example, a section close to the end of the panel will have less stiffness than a section on the center of the panel, provided the designer space all connectors evenly. For this case, the calculations require the computation of two stiffnesses, one for the shear force on the connector and one for the moment, axial force and deflection at midspan. On the other hand, if the engineer decides to use a wider separation of connectors near midspan, then the stiffness used in the calculations of forces and deformations should be the one at the end of the panel. These two cases can be expressed using the following equations:

$$\text{Stiffness at panel end: } K = \frac{\text{number of connectors} \times k_{conn}}{\text{width} \times (s/2 + \text{distance to end})} \quad (5-10)$$

$$\text{Stiffness at midspan: } K = \frac{\text{number of connectors} \times k_{conn}}{\text{width} \times (s)} \quad (5-11)$$

$$\chi = \sqrt{\frac{K(t_1 + t_2)}{t_1 t_2 E c}} \quad (5-12)$$

CHAPTER 6

CONCLUSIONS

6.1 Full Scale Testing

A concrete sandwich wall panel was tested at the Utah State University's Systems, Materials, and Structural Health (SMASH) Laboratory. The goal of this testing was to verify assumptions made by different researchers about the behavior of sandwich panels under thermal gradients. The following conclusions can be drawn based on the experimental results:

- The variation in temperature of the unheated wythe is negligible.
- The variation in temperature between two points within a wythe is minimal.
- Bowing is imperceptible in short SWPs, i.e., 15-ft. long panels.
- There is a linear relationship between bowing and the thermal gradient in the elastic range.

6.2 Parametric Analysis

A parametric analysis was performed in this section. This allowed us to identify the variables that affect thermal bowing within the scope of this research, and draw the following conclusions:

- The maximum connector rotation, axial and shear force, and the stresses on the wythes increase as the panel stiffness increase.

- For a given panel stiffness, the maximum connector shear and axial force is the same, regardless of the panel length.
- The maximum connector slip decreases as the panel stiffness increases.
- Bowing and the span length have a quadratic relationship.
- The distance between wythe's centroids and bowing have an inverse relation.
- The coefficient of thermal expansion and bowing have a linear relationship.
- The variation on compressive strength does not affect bowing significantly, however, an increase in compressive strength can avoid cracking.
- PCI handbook equation 5-81 yields higher deflections values than either FEA or Holmberg & Plem (1965) equation.

6.3 Serviceability Analysis

In this section, a procedure to consider thermal bowing as part of the serviceability checks was proposed based on the finite element results, the ACI 318-14(ACI Committee 318, 2014) design code and the PCI Handbook (PCI, 2010) recommendations for slenderness effects in columns and wall panels. A method for computing forces, moments, displacements for panels with thermal bowing was also developed.

6.4 Future Research

1. Further testing is required to determine the behavior of wall panels under the effects of thermal bowing and other type of loading.

2. Perform a reliability analysis to determine which load combinations require the inclusion of thermal gradients effects on SWPs.
3. Study the behavior of sandwich panels after cracking.
4. Perform an investigation to accurately determine the effective stiffness of sandwich wall panels.
5. Study the impact of thermal bridging on thermal bowing.
6. Investigate the effect of prestressing on thermal bowing.

REFERENCES

- ACI Committee 318. (2014). Building Code Requirements for Structural Concrete (ACI 318M-14), an ACI Standard, and Commentary on Building Code Requirements for Structural Concrete (ACI 318RM-14), an ACI report (p. 519). American Concrete Institute.
- Al-Rubaye, S., Sorensen, T., & Maguire, M. (2017). *Investigating Composite Action at Ultimate for Commercial Sandwich Panel Composite Connectors*.
- Balik, J., & Barney, G. (1985). Thermal Design of Precast Concrete Buildings. *PCI Journal*, 48–98.
- Collins, T. F. (1954). Precast Concrete Sandwich Panels for Tilt-Up Construction. *Journal of the American Concrete Institute*, 50(2), 149–164.
<https://doi.org/10.14359/11671>
- Einea, A. (1992). Structural and thermal efficiency of precast concrete sandwich panel systems.
- Einea, A., Salmon, D. C., Tadros, M. K., & Culp, T. D. (1997). Full Scale Testing of Precast Concrete Sandwich Panels. *Structural Journal*, 94(4), 354–362.
<https://doi.org/10.14359/486>
- Ghali, A., Favre, R., & Elbadry, M. (2002). *Concrete Structures, Stresses and Deformations*. London and New York: E & FN SPON.
- Granhölm, H. (1949). *Om sammansatta balkar och pelare med särskild hänsyn till spikade träkonstruktioner: On composite beams and columns with particular regard to nailed timber structures*. Elanders boktryckeri aktiebolag.

- Holmberg, A., & Plem, E. (1965). *Behaviour of load-bearing sandwich-type structures*. Byggforskningen.
- Leabu, V. F. (1960). Problems and Performance of Precast Concrete Wall Panels. *Journal of the American Concrete Institute*, 56(10), 287–298.
<https://doi.org/10.14359/8097>
- Lee, B.-J., & Pessiki, S. (2004). Analytical investigation of thermal performance of precast concrete three-wythe sandwich wall panels. *PCI Journal*, 49(4), 88–101.
- Leung, A. K.-K. (1984). Structural design and analysis of concrete sandwich panels and their practical applications. Memorial University of Newfoundland.
- Losch, E. D., Hynes, P. W., Andrews Jr, R., Browning, R., Cardone, P., Devalapura, R., ... Goettsche, G. (2011). State of the Art of Precast/Prestressed Concrete Sandwich Wall Panels. *PCI Journal*, 56(2), 131–176.
- McCall, W. C. (1985). Thermal Properties of Sandwich Panels. *Concrete International*, 35–41.
- Naito, C. J., Hoemann, J. M., Shull, J. S., Saucier, A., Salim, H. A., Bewick, B. T., & Hammons, M. I. (2011). *Precast/prestressed concrete experiments performance on non-load bearing sandwich wall panels*. BLACK AND VEATCH OVERLAND PARK KS.
- Nowak, A. S., & Collins, K. R. (2012). *Reliability of structures*. CRC Press.
- Olsen, J., Al-Rubaye, S., Sorensen, T., & Maguire, M. (2017). Developing a General Methodology for Evaluating Composite Action in Insulated Wall Panels.
- PCI. (2010). PCI Design Handbook, Precast and Prestressed Concrete. *Prestressed*

Concrete Institute,.

Powell, G. H. (2010). *Modeling for structural analysis: behavior and basics*. Computers and Structures.

Sorensen, T., Dorafshan, S., & Maguire, M. (2017, January 6). Thermal Evaluation of Common Locations of Heat Loss in Sandwich Wall Panels. *Congress on Technical Advancement 2017*. <https://doi.org/doi:10.1061/9780784481011.017>

Unnithan, G., KrishnaKumar, R., & Prasad, A. (2003). Application of a Shell-Spring Model for the Optimization of Radial Tire Contour Using a Genetic Algorithm. *Tire Science and Technology*, 31(1), 39–63. <https://doi.org/10.2346/1.2135261>

Zhu, W., Huang, Z., & Liang, J. (2006). Studies on shell-spring design model for segment of shield tunnels. *Yantu Gongcheng Xuebao(Chinese Journal of Geotechnical Engineering)*, 28(8), 940–947.

APPENDICES

APPENDIX A.

Derivation of Thermal Bowing Equations

A.1 Derivation of Equation (2-1)

Consider a sandwich panel subjected to a temperature differential over its, as shown on Figure 6-1.

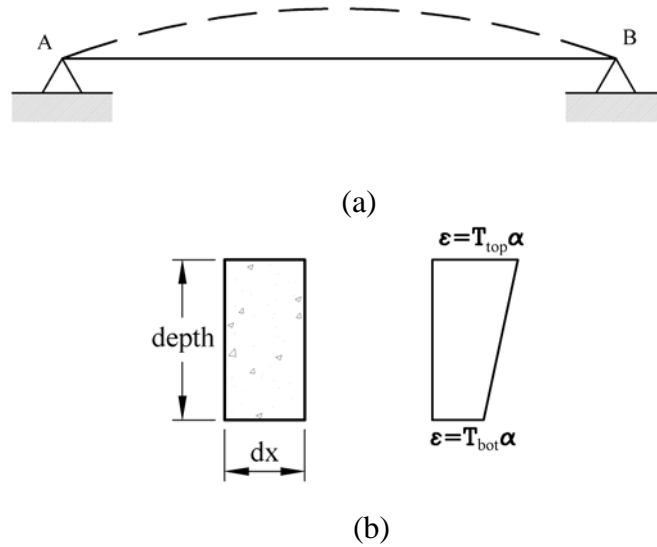


Figure 6-1 Panel subjected to a temperature differential

If take a differential element and compute the strain at an arbitrary location within the panel length, it yields:

$$\epsilon_{top} = \frac{\alpha T_{top} dx}{dx} = \alpha T_{top} \quad (A.1-1)$$

$$\epsilon_{bot} = \frac{\alpha T_{bot} dx}{dx} = \alpha T_{bot} \quad (A.1-2)$$

And the curvature is as follow:

$$\frac{1}{\rho} = \frac{\epsilon_m}{d} = \frac{\alpha(T_{top} - T_{bot})}{d} \quad (A.1-3)$$

Also,

$$\frac{d^2 y}{dx^2} = \frac{\alpha(T_{top} - T_{bot})}{d} \quad (A.1-4)$$

Integrating equation (A.1-4):

$$\theta = \frac{\alpha(T_{top} - T_{bot})}{d}x + C_1 \quad (A.1-5)$$

And,

$$y = \frac{\alpha(T_{top} - T_{bot})}{2d}x^2 + C_1x + C_2 \quad (A.1-6)$$

By using the boundary conditions $\theta = 0$ when $x = L/2$, and $y = 0$ when $x = 0$, it gives:

$$\theta = \frac{\alpha(T_{top} - T_{bot})}{d}x - \frac{\alpha(T_{top} - T_{bot})L}{2d} \quad (A.1-7)$$

$$y = \frac{\alpha(T_{top} - T_{bot})}{2d}x^2 - \frac{\alpha(T_{top} - T_{bot})L}{2d}x \quad (A.1-8)$$

Which evaluated at midspan yields the equation (2-1):

$$y = \frac{\alpha(T_{top} - T_{bot})}{8d}L^2$$

A.2 Derivation of Equation (5-9)

If we take the nailed sandwich beam theory from Granholm (1949), and apply it to sandwich wall panels of different wythe thickness and the same modulus of elasticity, we have the following:

$$\varphi'' - \chi^2\varphi = (r_1 + r_2)v''' \quad (A.2-9)$$

$$v'' - \frac{\alpha^2}{r_1 + r_2}\varphi' = -\frac{M_x}{EI} \quad (A.2-10)$$

These equations were extended to sandwich panels by Holmberg & Plem (1965), and equation (A.2-10) was modified to include the temperature differential as follow:

$$v'' - \frac{\alpha^2}{r_1 + r_2} \varphi' = \frac{\alpha^2}{r_1 + r_2} \mu t \quad (A.2-11)$$

By using the boundary conditions⁵ $\varphi = 0$ when $x = 0$, and $v'' = 0$ when $x = L/2$, it yields:

$$\varphi = -c \times \Delta T \frac{\beta}{\chi} \left(\frac{\sinh \frac{\chi}{\beta} x}{\cosh \frac{\chi l}{2\beta}} \right) \quad (A.2-12)$$

$$F_{shear} = \varphi k_{conn} \quad (A.2-13)$$

Also, using the concept of equilibrium, $M_1 + M_2 + (r_1 + r_2)N = 0$, we find:

$$M_1 = -\frac{\alpha^2}{r_1 + r_2} c \times \Delta T \times E_c \times i_1 \left(1 - \frac{\cosh \frac{\chi}{\beta} x}{\cosh \frac{\chi l}{2\beta}} \right) \quad (A.2-14)$$

$$M_2 = -\frac{\alpha^2}{r_1 + r_2} c \times \Delta T \times E_c \times i_2 \left(1 - \frac{\cosh \frac{\chi}{\beta} x}{\cosh \frac{\chi l}{2\beta}} \right) \quad (A.2-15)$$

$$N = -\frac{\alpha^2}{(r_1 + r_2)^2} c \times \Delta T \times E_c \times I_{NC} \left(1 - \frac{\cosh \frac{\chi}{\beta} x}{\cosh \frac{\chi l}{2\beta}} \right) \quad (A.2-16)$$

⁵ For these equations, midspan is at $x = 0$ and $\pm L/2$ represents the panel supports.

Finally, after substituting equation (A.2-12) in equation (A.2-11), and integrating twice we get:

$$v = +\frac{1}{8} \times \mu t \times \frac{l^2}{r} \times \alpha^2 \left[\left(\frac{2\beta}{\kappa l} \right)^2 \times \left(1 - \frac{\cosh \frac{\kappa}{\beta} x}{\cosh \frac{\kappa l}{2\beta}} \right) - \frac{1}{2} \left(1 - \left(\frac{2x}{l} \right)^2 \right) \right]$$

APPENDIX B.

Thermal Bowing Application Examples

B.1 Example 1: A concrete sandwich wall panel with

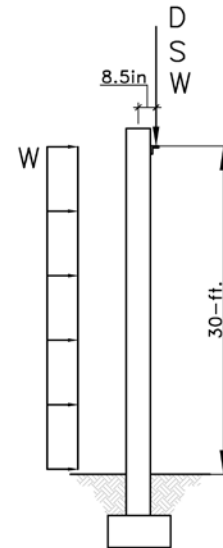
Example B1. Partially Composite Bearing Panel

Consider a 30-ft. span long concrete sandwich wall panel with a 3-2-3 configuration, which has been designed to resist wind, snow, live and dead load. The panel was not designed for thermal gradients. These loads are:

$$D := 1 \text{ klf} \quad S := 0.75 \text{ klf} \quad \Delta T := 50 \text{ F}$$

$$e_p := 8.5 \text{ in} \quad W := -0.325 \frac{\text{klf}}{\text{ft}} \quad (\text{Roof Suction})$$

$$W_p := 0.12 \frac{\text{klf}}{\text{ft}} \quad l := 30 \text{ ft}$$



The panel properties are:

$$f'_c := 4 \text{ ksi} \quad E_c := 57000 \cdot \sqrt{f'_c \cdot \text{psi}} = 3605 \text{ ksi} \quad c := \frac{5.5 \cdot 10^{-6}}{F}$$

$$t_1 := 3 \text{ in} \quad t_2 := 3 \text{ in} \quad t_{ins} := 5 \text{ in} \quad w := 96 \text{ in} \quad w_{panel} := 0.6 \text{ klf}$$

$$s_x := 24 \text{ in} \quad d_{conn_border} := 12 \text{ in} \quad s_y := 48 \text{ in} \quad k_{conn} := 400 \frac{\text{kip}}{\text{in}}$$

I. Compute panel forces, moments and deformations:

I.a Compute panel stiffness:

$$K := \frac{k_{conn}}{s_x \cdot s_y} = 347.222 \frac{\text{lb}}{\text{in}^3}$$

I.b Compute panel percentage of composite action and effective moment of inertia:

$$y_{cg} := \frac{\frac{t_1^2}{2} + t_2 \cdot \left(\frac{t_2}{2} + t_{ins} + t_1 \right)}{t_1 + t_2} = 5.5 \text{ in}$$

$$r_1 := y_{cg} - \frac{t_1}{2} = 4 \text{ in} \quad r_2 := t_1 + t_{ins} + \frac{t_2}{2} - y_{cg} = 4 \text{ in}$$

$$A_1 := w \cdot t_1 = 288 \text{ in}^2$$

$$A_2 := w \cdot t_2 = 288 \text{ in}^2$$

$$i_1 := w \cdot \frac{t_1^3}{12} = 216 \text{ in}^4$$

$$i_2 := w \cdot \frac{t_2^3}{12} = 216 \text{ in}^4$$

$$I_{NC} := i_1 + i_2 = 432 \text{ in}^4$$

$$I_{FC} := I_{NC} + A_1 \cdot r_1^2 + A_2 \cdot r_2^2 = (9.648 \cdot 10^3) \text{ in}^4$$

$$\alpha := \sqrt{\frac{I_{FC} - I_{NC}}{I_{FC}}} = 0.977$$

$$\beta := \sqrt{\frac{I_{NC}}{I_{FC}}} = 0.212$$

$$\omega := \sqrt{\frac{K \cdot (t_1 + t_2)}{E_c \cdot t_1 \cdot t_2}} = 0.0080132 \frac{1}{\text{in}}$$

$$PCA := 1 - 2 \left(2 \frac{\beta}{\omega \cdot l} \right)^2 \cdot \left(1 - \operatorname{sech} \left(\frac{\omega \cdot l}{2 \beta} \right) \right) = 0.957$$

$$I_{eff} := I_{NC} + (I_{FC} - I_{NC}) \cdot PCA = 9252.17 \text{ in}^4$$

Compute the moment and axial force on each wythe:

$$x := \begin{bmatrix} 14 \\ 10 \\ 6 \\ 2 \\ 0 \end{bmatrix} \text{ ft} \quad v'' := -\frac{\alpha^2 \cdot c \cdot \Delta T}{r_1 + r_2} \cdot \left(1 - \frac{\cosh \left(\frac{\omega \cdot x}{\beta} \right)}{\cosh \left(\frac{\omega \cdot l}{2 \beta} \right)} \right) = \begin{bmatrix} -1.199 \cdot 10^{-5} \\ -2.945 \cdot 10^{-5} \\ -3.228 \cdot 10^{-5} \\ -3.273 \cdot 10^{-5} \\ -3.276 \cdot 10^{-5} \end{bmatrix} \frac{1}{\text{in}}$$

$$M_1 := -v'' \cdot E_c \cdot i_1 = \begin{bmatrix} 9.337 \\ 22.932 \\ 25.139 \\ 25.488 \\ 25.513 \end{bmatrix} \text{ kip} \cdot \text{in}$$

$$M_{unit_11} := \frac{M_1}{w} = \begin{bmatrix} 0.097 \\ 0.239 \\ 0.262 \\ 0.265 \\ 0.266 \end{bmatrix} \text{ in} \cdot \frac{\text{kip}}{\text{in}}$$

$$M_2 := -v'' \cdot E_c \cdot i_2 = \begin{bmatrix} 9.337 \\ 22.932 \\ 25.139 \\ 25.488 \\ 25.513 \end{bmatrix} \text{ kip} \cdot \text{in}$$

$$M_{unit_11} := \frac{M_2}{w} = \begin{bmatrix} 0.097 \\ 0.239 \\ 0.262 \\ 0.265 \\ 0.266 \end{bmatrix} \text{ in} \cdot \frac{\text{kip}}{\text{in}}$$

$$N := \frac{M_1 + M_2}{r_1 + r_2} = \begin{bmatrix} 2.334 \\ 5.733 \\ 6.285 \\ 6.372 \\ 6.378 \end{bmatrix} \text{ kip}$$

$$N_{unit} := \frac{N}{w} = \begin{bmatrix} 0.024 \\ 0.06 \\ 0.065 \\ 0.066 \\ 0.066 \end{bmatrix} \frac{\text{kip}}{\text{in}}$$

Compute the stresses on the wythes

Sun exposed wythe:

$$\sigma_1 := \frac{N}{A_1} + \frac{M_1 \cdot \frac{t_1}{2}}{i_1} = \begin{bmatrix} 0.057 \\ 0.139 \\ 0.153 \\ 0.155 \\ 0.155 \end{bmatrix} \text{ ksi}$$

$$\sigma_2 := \frac{N}{A_1} - \frac{M_1 \cdot \frac{t_1}{2}}{i_1} = \begin{bmatrix} -0.073 \\ -0.179 \\ -0.196 \\ -0.199 \\ -0.199 \end{bmatrix} \text{ ksi}$$

Inner building wythe:

$$\sigma_3 := \frac{N}{A_1} + \frac{M_1 \cdot \frac{t_1}{2}}{i_1} = \begin{bmatrix} 0.073 \\ 0.179 \\ 0.196 \\ 0.199 \\ 0.199 \end{bmatrix} \text{ ksi}$$

$$\sigma_3 := \frac{N}{A_2} - \frac{M_2 \cdot \frac{t_2}{2}}{i_2} = \begin{bmatrix} -0.057 \\ -0.139 \\ -0.153 \\ -0.155 \\ -0.155 \end{bmatrix} \text{ ksi}$$

Case 1: Service I = D + T

Find the deflection due to dead load and the thermal gradient.

Compute the deflection due to the thermal gradient:

$$P_{D_top} := w \cdot D = 8 \text{ kip} \quad P_{D_mid} := P_{D_top} + w_{panel} \cdot \frac{l}{2} = 17 \text{ kip}$$

Compute the effective stiffness of the panel for dead load:

$$I_{eff} := I_{NC} + PCA \cdot (I_{FC} - I_{NC}) = 9252.17 \text{ in}^4 \quad \phi_k := 0.85 \quad \beta_d := 1 \quad (\text{Only dead load})$$

$$EI_{effD} := \frac{\phi_k \cdot E_c \cdot I_{eff}}{1 + \beta_d} = (1.418 \cdot 10^7) \text{ kip} \cdot \text{in}^2$$

Calculate the deflection at mid-height:

$$\Delta_D := \frac{P_{D_top} \cdot e_p \cdot l^2}{16 EI_{effD}} = 0.039 \text{ in}$$

Find the deflection due to temperature:

$$\Delta_{\Delta T} := -\frac{1}{4} \cdot c \cdot \Delta T \cdot \frac{l^2}{r_1 + r_2} \cdot \alpha^2 \cdot \left(\left(2 \frac{\beta}{\omega \cdot l} \right)^2 \cdot \left(1 - \operatorname{sech} \left(\frac{\omega \cdot l}{2 \beta} \right) \right) - 0.5 \right) = 0.509 \text{ in}$$

Estimate the initial bow:

$$\Delta_{\text{bow}} := \frac{l}{360} = 1 \text{ in}$$

Total deflection (bow, temperature and dead load):

$$\Delta_{\text{initial}} := \Delta_{\text{bow}} + \Delta_{\Delta T} + \Delta_D = 1.548 \text{ in}$$

Perform a P-Delta analysis:

$$\Delta := \frac{P_{D_mid} \cdot l^2}{8 EI_{effD}} = 0.019$$

First Iteration:

$$e_1 := \Delta_{\text{initial}} = 1.548 \text{ in}$$

$$\Delta_1 := \Delta \cdot e_1 = 0.0301 \text{ in}$$

Second Iteration:

$$e_2 := e_1 + \Delta_1 = 1.578 \text{ in}$$

$$\Delta_2 := \Delta \cdot e_2 = 0.0307 \text{ in}$$

Third Iteration:

$$e_3 := e_1 + \Delta_2 = 1.579 \text{ in}$$

$$\Delta_3 := \Delta \cdot e_3 = 0.0307 \text{ in}$$

Fourth Iteration:

$$e_4 := e_1 + \Delta_3 = 1.579 \text{ in} < \frac{l}{150} = 2.4 \text{ in}$$

$$\Delta_4 := \Delta \cdot e_4 = 0.0307 \text{ in} \quad (\text{Converge})$$

Case 2: $Service\ 2 = D + 0.75(W+T)$

Find the deflection due to dead load, wind load and the thermal gradient.

Compute the deflection due to wind:

$$\phi_k := 0.85 \quad \beta_d := 0 \quad (\text{Wind Load})$$

$$EI_{effW} := \frac{\phi_k \cdot E_c \cdot I_{eff}}{1 + \beta_d} = (2.835 \cdot 10^7) \text{ kip} \cdot \text{in}^2$$

$$W_p := W_p \cdot w = 0.96 \text{ klf} \quad \Delta_W := \frac{5}{385} \cdot \frac{W_p \cdot l^4}{EI_{effW}} = 0.616 \text{ in}$$

Total deflection (bow, wind, temperature and dead load):

$$\Delta_{initial} := \Delta_D + \Delta_{bow} + 0.75 \cdot (\Delta_{\Delta T} + \Delta_W) = 1.882 \text{ in}$$

Perform a P-Delta analysis:

$$\Delta := \frac{P_{D_mid} \cdot l^2}{8 EI_{effD}} = 0.019$$

First Iteration:

$$e_1 := \Delta_{initial} = 1.882 \text{ in}$$

$$\Delta_1 := \Delta \cdot e_1 = 0.0366 \text{ in}$$

Second Iteration:

$$e_2 := e_1 + \Delta_1 = 1.919 \text{ in}$$

$$\Delta_2 := \Delta \cdot e_2 = 0.0373 \text{ in}$$

Third Iteration:

$$e_3 := e_1 + \Delta_2 = 1.92 \text{ in} \quad < \frac{l}{150} = 2.4 \text{ in}$$

$$\Delta_3 := \Delta \cdot e_3 = 0.0373 \text{ in} \quad (\text{Converge})$$

APPENDIX C.

VBA Code for Parametric Analysis

'Option Explicit allow only declared variables to be used

Option Explicit

'Dimensioning variables so that they may be used anywhere in the module

'Also declaring SApObjet with application and class type so that early biding occurs

'dimension variables

Dim SapObject As SAP2000v18.cOAPI

Dim Helper As SAP2000v18.cHelper

Dim SapModel As cSapModel

Dim ret As Long

Dim lengths As Range

Dim coordinates As Range

Sub Sap2000_open()

'Create the SAP2000 Object

Set Helper = New SAP2000v18.Helper

Set SapObject = Helper.CreateObject("C:\Program Files\Computers and
Structures\SAP2000 18\sap2000.exe")

'Start the Sap2000 application

SapObject.ApplicationStart

'Initialize model

SapObject.SapModel.InitializeNewModel (eUnits_kip_in_F)

'Create a blank model

SapObject.SapModel.File.NewBlank

End Sub

Sub Sap2000_build()

'Dimensioning variables for this sub

Dim totalRows As Integer

Dim rowNumber As Integer

Dim xCoord1 As Double

Dim xCoord2 As Double

Dim Name As String

Dim i As Integer

Dim j As Integer

Dim restraintValue() As Boolean

Dim NumberObjects As Long

Dim ObjectName() As String

Dim ObjectType() As Long

Dim Value() As Boolean

Dim DOF() As Boolean

Dim Fixed() As Boolean

Dim Ke() As Double

Dim Ce() As Double

Dim NumberAreas As Long

Dim AreaName() As String

Dim fconn As Double

Dim Num As Long

Dim NewName() As String

Dim Sadj As Double

Dim nA As Long

Dim Srow As Double

Dim NumberNames As Long

Dim MyName() As String

Dim ConnCol As Long

Dim t1 As Double

Dim t2 As Double

Dim ins As Double

Dim dist As Double

Dim panellength As Double

'Determine the number of rows in the range

```
totalRows = 8
```

'Define Link

```
ReDim DOF(5)
```

```
ReDim Fixed(5)
```

```
ReDim Ke(5)
```

```
ReDim Ce(5)
```

```
For i = 0 To 2
```

```
    DOF(i) = True
```

```
    Ce(i) = True
```

```
Next i
```

```
Ke(0) = Sheets("PANEL_INFO").Cells(8, 2).Value
```

```
Ke(1) = Sheets("PANEL_INFO").Cells(9, 2).Value
```

```
Ke(2) = Sheets("PANEL_INFO").Cells(10, 2).Value
```

```
Ce(0) = Ke(0)
```

```
Ce(1) = Ke(1)
```

```
Ce(2) = Ke(2)
```

```
ret = SapObject.SapModel.PropLink.SetLinear("L1", DOF, Fixed, Ke, Ce, 0, 0)
```

'Create Panels

```
fconn = Sheets("PANEL_INFO").Cells(11, 2).Value
```

```
Dim frameName(0) As String
```

```
xCoord1 = fconn
```

```
xCoord2 = Sheets("PANEL_INFO").Cells(12, 2).Value
```

```
Srow = Sheets("PANEL_INFO").Cells(3, 6).Value
```

```
Num = Sheets("PANEL_INFO").Cells(7, 2).Value
```

```
t1 = Sheets("PANEL_INFO").Cells(3, 2).Value
```

```
t2 = Sheets("PANEL_INFO").Cells(4, 2).Value
```

```
ins = Sheets("PANEL_INFO").Cells(5, 2).Value
```

```
dist = t1 / 2 + t2 / 2 + ins
```

'Do a loop so all panels are generated automatically by the API

```
For i = 1 To totalRows
```

```
panellength = Sheets("PANEL_INFO").Cells(i + 2, 4).Value
```

```
Sadj = Sheets("PANEL_INFO").Cells(i + 2, 5).Value
```

```
ConnCol = (panellength - 2 * fconn) / Sadj + 1
```

```
ret = SapObject.SapModel.FrameObj.AddByCoord((i - 1) * (xCoord2 + 12), 0, -  
fconn, fconn + (i - 1) * (xCoord2 + 12), 0, -fconn, Name)
```

```

ret = SapObject.SapModel.FrameObj.AddByCoord(xCoord1 + (i - 1) * (xCoord2
+ 12), 0, -fconn, xCoord1 + Srow + (i - 1) * (xCoord2 + 12), 0, -fconn, Name)

ret = SapObject.SapModel.FrameObj.GetNameList(NumberNames, MyName)

For j = 0 To (NumberNames - 1)

ret = SapObject.SapModel.EditGeneral.ExtrudeFrameToAreaLinear(MyName(j),
"Default", 0, 0, fconn, 1, AreaName, True)

Next j

ret = SapObject.SapModel.FrameObj.AddByCoord((i - 1) * (xCoord2 + 12), 0, 0,
fconn + (i - 1) * (xCoord2 + 12), 0, 0, Name)

ret = SapObject.SapModel.FrameObj.AddByCoord(xCoord1 + (i - 1) * (xCoord2
+ 12), 0, 0, xCoord1 + Srow + (i - 1) * (xCoord2 + 12), 0, 0, Name)

ret = SapObject.SapModel.FrameObj.GetNameList(NumberNames, MyName)

For j = 0 To (NumberNames - 1)

ret = SapObject.SapModel.EditGeneral.ExtrudeFrameToAreaLinear(MyName(j),
"Default", 0, 0, Sadj, ConnCol - 1, AreaName, True)

Next j

```

'Replicate Shell elements for panel core

```
ret = SapObject.SapModel.SelectObj.CoordinateRange(xCoord1 + (i - 1) *
(xCoord2 + 12), xCoord1 + Srow + (i - 1) * (xCoord2 + 12), 0, 0, -fconn, panellength, , ,
, False, False, True, False, False)
```

```
ret = SapObject.SapModel.EditGeneral.ReplicateLinear(Srow, 0, 0, Num - 2,
NumberObjects, ObjectName, ObjectType)
```

```
ret = SapObject.SapModel.SelectObj.ClearSelection
```

'Replicate Shell elements for vertical border

```
ret = SapObject.SapModel.SelectObj.CoordinateRange((i - 1) * (xCoord2 + 12),
xCoord1 + (i - 1) * (xCoord2 + 12), 0, 0, -fconn, panellength - 2 * fconn, , , False, False,
True, False, False)
```

```
ret = SapObject.SapModel.EditGeneral.ReplicateLinear(xCoord2 - xCoord1, 0, 0,
1, NumberObjects, ObjectName, ObjectType)
```

```
ret = SapObject.SapModel.SelectObj.ClearSelection
```

'Replicate Shell elements for horizontal border

```
ret = SapObject.SapModel.SelectObj.CoordinateRange((i - 1) * (xCoord2 + 12),
xCoord2 + (i - 1) * (xCoord2 + 12), 0, 0, -fconn, 0, , , False, False, True, False, False)
```

```
ret = SapObject.SapModel.EditGeneral.ReplicateLinear(0, 0, panellength - fconn,
1, NumberObjects, ObjectName, ObjectType)
```

```
ret = SapObject.SapModel.SelectObj.ClearSelection
```


'Add second panel

```
ret = SapObject.SapModel.SelectObj.CoordinateRange((i - 1) * (xCoord2 + 12),
xCoord2 + (i - 1) * (xCoord2 + 12), 0, 0, -fconn, panellength, , , False, False, True,
False, False)
```

```
ret = SapObject.SapModel.EditGeneral.ReplicateLinear(0, dist, 0, 1,
NumberObjects, ObjectName, ObjectType)
```

```
ret = SapObject.SapModel.View.RefreshView(0, "False")
```

```
ret = SapObject.SapModel.SelectObj.ClearSelection
```

'Refresh view

```
ret = SapObject.SapModel.View.RefreshView(0, "False")
```

'Add link object by coordinate

```
ret = SapObject.SapModel.LinkObj.AddByCoord(fconn + (i - 1) * (xCoord2 +
12), 0, 0, fconn + (i - 1) * (xCoord2 + 12), dist, 0, 1, False, "L1")
```

```
ret = SapObject.SapModel.SelectObj.CoordinateRange(0 + (i - 1) * (xCoord2 +
12), xCoord2 + (i - 1) * (xCoord2 + 12), 0, dist, 0, 0, False, , True, False, False, False,
False, True)
```

```
ret = SapObject.SapModel.EditGeneral.ReplicateLinear(Srow, 0, 0, Num - 1,
NumberObjects, ObjectName, ObjectType)
```

```
ret = SapObject.SapModel.SelectObj.ClearSelection
```

```
ret = SapObject.SapModel.SelectObj.CoordinateRange(0 + (i - 1) * (xCoord2 +
12), xCoord2 + (i - 1) * (xCoord2 + 12), 0, dist, 0, panellength, False, , True, False, False,
False, False, True)
```

```
ret = SapObject.SapModel.EditGeneral.ReplicateLinear(0, 0, Sadj, ConnCol - 1,
NumberObjects, ObjectName, ObjectType)
```

```
ret = SapObject.SapModel.SelectObj.ClearSelection
```

```
Next i
```

'Modify Shell Properties

```
ret = SapObject.SapModel.PropArea.SetShell("ASEC1", 1, "4000Psi", 0, t1, t1)
```

```
ret = SapObject.SapModel.PropArea.SetShell_1("ASEC2", 1, True, "4000Psi", 0, t2,
t2)
```

```
ret = SapObject.SapModel.SelectObj.CoordinateRange(0, totalRows * (xCoord2 +
12), 0, 0, -fconn, panellength, , , True, False, False, True, False, False)
```

```
ret = SapObject.SapModel.AreaObj.SetProperty(Name, "ASEC2",
eItemType_SelectedObjects)
```

'Clear Selection

```
ret = SapObject.SapModel.SelectObj.ClearSelection
```

'Define Thermal Load Patterns

```
Dim tempload() As Variant
```

```

Dim T() As Variant

T = Sheets("PANEL_INFO").Range("H3:H12").Value

tempload = Sheets("PANEL_INFO").Range("I3:I12").Value

For i = 1 To 10

    ret = SapObject.SapModel.LoadPatterns.Add(T(i, 1),
eLoadPatternType_Temperature, 0)

    ret = SapObject.SapModel.SelectObj.CoordinateRange(0, totalRows * (xCoord2
+ 12), 1, dist + 1, -fconn, panellength + 1, , , True, , , True)

    ret = SapObject.SapModel.AreaObj.SetLoadTemperature("ASEC1", T(i, 1), 1,
tempload(i, 1), , , eItemType_SelectedObjects)

    ret = SapObject.SapModel.SelectObj.ClearSelection

Next i

'Add full fixity restraints at end joints

ReDim restraintValue(5)

For i = 0 To 2

    restraintValue(i) = True

Next i

ret = SapObject.SapModel.SelectObj.CoordinateRange(0, totalRows * (xCoord2 +
12), 0, 0, 0, 0, , , True, True, False, False, False, False)

```

```

    ret = SapObject.SapModel.PointObj.SetRestraint(Name, restraintValue,
eItemType_SelectedObjects)

    ret = SapObject.SapModel.SelectObj.ClearSelection

    restraintValue(0) = False

    restraintValue(2) = False

For i = 1 To totalRows

    panellength = Sheets("PANEL_INFO").Cells(i + 2, 4).Value

    Sadj = Sheets("PANEL_INFO").Cells(i + 2, 5).Value

    ConnCol = (panellength - 2 * fconn) / Sadj + 1

    ret = SapObject.SapModel.SelectObj.CoordinateRange((i - 1) * (xCoord2 + 12), i
* (xCoord2) + 12 * (i - 1), 0, 0, panellength - 2 * fconn, panellength - 2 * fconn, , , True,
True, False, False, False, False)

    ret = SapObject.SapModel.PointObj.SetRestraint(Name, restraintValue,
eItemType_SelectedObjects)

    ret = SapObject.SapModel.SelectObj.ClearSelection

Next i

End Sub

```

```
Sub Sap2000_set_mesh()
```

```
'assign auto mesh options
```

```
    ret = SapObject.SapModel.SelectObj.All
```

```
    ret = SapObject.SapModel.AreaObj.SetAutoMesh("ALL", 6, , , , , , , 12, , , , , , ,
```

```
eItemType_SelectedObjects)
```

```
End Sub
```

```
Sub Sap2000_run()
```

```
'Dimensioning variables for this sub
```

```
    Dim nameofmodel As String
```

```
    nameofmodel = Sheets("PANEL_INFO").Cells(15, 2).Value
```

```
'Save model
```

```
    ret = SapObject.SapModel.File.Save(nameofmodel)
```

```
'Run model (this will create the analysis model from the object model)
```

```
    ret = SapObject.SapModel.Analyze.RunAnalysis
```

```
End Sub
```

```
Sub Sap2000_get_data()
```

```
'Dimensioning variables for this sub
```

```
Dim numberResults As Long
```

```
Dim Obj() As String
```

```
Dim Elm() As String
```

```
Dim LoadCase() As String
```

```
Dim stepType() As String
```

```
Dim stepNum() As Double
```

```
Dim u1() As Double
```

```
Dim u2() As Double
```

```
Dim u3() As Double
```

```
Dim r1() As Double
```

```
Dim r2() As Double
```

```
Dim r3() As Double
```

```
Dim i As Integer
```

```
Dim r As Integer
```

```
Dim Joint As String
```

```
Dim Row As Integer
```

```
Dim NumJoint As String
```

```
Dim LinkObj As String
```

```
Dim p() As Double
```

Dim V2() As Double
Dim V3() As Double
Dim T() As Double
Dim M2() As Double
Dim M3() As Double
Dim PointElm() As String
Dim Link As String
Dim NumLink As String
Dim S11Top() As Double
Dim S22Top() As Double
Dim S12Top() As Double
Dim SMaxTop() As Double
Dim SMinTop() As Double
Dim SAngleTop() As Double
Dim SVMTop() As Double
Dim S11Bot() As Double
Dim S22Bot() As Double
Dim S12Bot() As Double
Dim SMaxBot() As Double
Dim SMinBot() As Double
Dim SAngleBot() As Double
Dim SVMBot() As Double

Dim S13Avg() As Double

Dim S23Avg() As Double

Dim SMaxAvg() As Double

Dim SAngleAvg() As Double

Dim NumShell As String

Dim ShellStress As String

Dim panellength As Double

Dim xCoord2 As Double

Dim fconn As Double

Dim Name As String

Dim Temp As String

Dim x As Integer

Dim t1 As Double

Dim t2 As Double

Dim dist As Double

Dim rot1 As Variant

Dim rot2 As Variant

Dim ins As Double

Dim Srow As Double

Dim Sadj As Double

Dim x1 As Double

Dim x2 As Double

'Write displacement results back into worksheet

```
xCoord2 = Sheets("PANEL_INFO").Cells(12, 2).Value
```

```
fconn = Sheets("PANEL_INFO").Cells(11, 2).Value
```

```
t1 = Sheets("PANEL_INFO").Cells(3, 2).Value
```

```
t2 = Sheets("PANEL_INFO").Cells(4, 2).Value
```

```
ins = Sheets("PANEL_INFO").Cells(5, 2).Value
```

```
dist = t1 / 2 + t2 / 2 + ins
```

```
Srow = Sheets("PANEL_INFO").Cells(3, 6).Value
```

```
For r = 1 To 8
```

```
    ret = SapObject.SapModel.Results.Setup.DeselectAllCasesAndCombosForOutput
```

```
    panellength = Sheets("PANEL_INFO").Cells(r + 2, 4).Value
```

```
    Sadj = Sheets("PANEL_INFO").Cells(r + 2, 5).Value
```

```
    x1 = xCoord2 / 2 - Srow + (r - 1) * (xCoord2 + 12)
```

```
    x2 = xCoord2 / 2 + Srow + (r - 1) * (xCoord2 + 12)
```

```
For i = 1 To 10
```

```
    Temp = Sheets("PANEL_INFO").Cells(i + 2, 8).Value
```

```
    ret = SapObject.SapModel.Results.Setup.SetCaseSelectedForOutput(Temp)
```

```
    ret = SapObject.SapModel.SelectObj.CoordinateRange(x1, x2, dist, dist, -fconn,
```

```
panellength, , , True, True, False, False, False, False)
```

```

ret = SapObject.SapModel.Results.JointDispl("ALL",
eItemTypeElm_SelectionElm, numberResults, Obj, Elm, LoadCase, stepType, stepNum,
u1, u2, u3, r1, r2, r3)

Worksheets("PANEL_INFO").Cells(i + 1, 11 + 11 * (r - 1)) =
Application.WorksheetFunction.Max(u2)

Worksheets("PANEL_INFO").Cells(i + 1, 20 + 11 * (r - 1)) = u3(numberResults -
2)

rot1 = r1(numberResults - 2)

ret = SapObject.SapModel.SelectObj.ClearSelection

ret = SapObject.SapModel.SelectObj.CoordinateRange(x1, x2, dist, dist,
(panellength - 2 * fconn) / 2 - 2 * Sadj, (panellength - 2 * fconn) / 2 + 2 * Sadj, , , True,
False, False, , False, False)

ret = SapObject.SapModel.Results.AreaStressShell("ALL",
eItemTypeElm_SelectionElm, numberResults, Obj, Elm, PointElm, LoadCase, stepType,
stepNum, S11Top, S22Top, S12Top, SMaxTop, SMinTop, SAngleTop, SVMTop,
S11Bot, S22Bot, S12Bot, SMaxBot, SMinBot, SAngleBot, SVMBot, S13Avg, S23Avg,
SMaxAvg, SAngleAvg)

Worksheets("PANEL_INFO").Cells(i + 1, 13 + 11 * (r - 1)) =
Application.WorksheetFunction.Max(S22Bot)

Worksheets("PANEL_INFO").Cells(i + 1, 14 + 11 * (r - 1)) =
Application.WorksheetFunction.Min(S22Top)

```

```
ret = SapObject.SapModel.SelectObj.ClearSelection
```

```
Temp = Sheets("PANEL_INFO").Cells(i + 2, 8).Value
```

```
ret = SapObject.SapModel.Results.Setup.SetCaseSelectedForOutput(Temp)
```

```
ret = SapObject.SapModel.SelectObj.CoordinateRange(x1, x2, 0, dist, -fconn,  
panellength, , , True, False, False, False, False, True)
```

```
ret = SapObject.SapModel.Results.LinkForce("ALL",
```

```
eItemTypeElm_SelectionElm, numberResults, Obj, Elm, PointElm, LoadCase, stepType,  
stepNum, p, V2, V3, T, M2, M3)
```

```
Worksheets("PANEL_INFO").Cells(i + 1, 17 + 11 * (r - 1)) =
```

```
Application.WorksheetFunction.Max(V2)
```

```
Worksheets("PANEL_INFO").Cells(i + 1, 18 + 11 * (r - 1)) =
```

```
Application.WorksheetFunction.Max(p)
```

```
ret = SapObject.SapModel.SelectObj.ClearSelection
```

```
Temp = Sheets("PANEL_INFO").Cells(i + 2, 8).Value
```

```
ret = SapObject.SapModel.Results.Setup.SetCaseSelectedForOutput(Temp)
```

```
ret = SapObject.SapModel.SelectObj.CoordinateRange(x1, x2, 0, 0, -fconn,  
panellength, , , True, False, False, False, False)
```

```
ret = SapObject.SapModel.Results.JointDispl("ALL",
```

```
eItemTypeElm_SelectionElm, numberResults, Obj, Elm, LoadCase, stepType, stepNum,  
u1, u2, u3, r1, r2, r3)
```

```

Worksheets("PANEL_INFO").Cells(i + 1, 12 + 11 * (r - 1)) =
Application.WorksheetFunction.Max(u2)

rot2 = r1(numberResults - 2)

ret = SapObject.SapModel.SelectObj.ClearSelection

ret = SapObject.SapModel.SelectObj.CoordinateRange(x1, x2, 0, 0, (panellength
- 2 * fconn) / 2 - 2 * Sadj, (panellength - 2 * fconn) / 2 + 2 * Sadj, , , True, False, False, ,
False, False)

ret = SapObject.SapModel.Results.AreaStressShell("ALL",
eItemTypeElm_SelectionElm, numberResults, Obj, Elm, PointElm, LoadCase, stepType,
stepNum, S11Top, S22Top, S12Top, SMaxTop, SMinTop, SAngleTop, SVMTop,
S11Bot, S22Bot, S12Bot, SMaxBot, SMinBot, SAngleBot, SVMBot, S13Avg, S23Avg,
SMaxAvg, SAngleAvg)

Worksheets("PANEL_INFO").Cells(i + 1, 15 + 11 * (r - 1)) =
Application.WorksheetFunction.Max(S22Bot)

Worksheets("PANEL_INFO").Cells(i + 1, 16 + 11 * (r - 1)) =
Application.WorksheetFunction.Min(S22Top)

ret = SapObject.SapModel.SelectObj.ClearSelection

Worksheets("PANEL_INFO").Cells(i + 1, 19 + 11 * (r - 1)) = rot1 - rot2

Next i

Next r

End Sub

```

```
Sub Change_Stiffness_of_Connectors()  
  
    ret = SapObject.SapModel.SetModelIsLocked(False)  
  
    Dim DOF() As Boolean  
  
    Dim Fixed() As Boolean  
  
    Dim Ke() As Double  
  
    Dim Ce() As Double  
  
    Dim j As Integer  
  
    ReDim DOF(5)  
  
    ReDim Fixed(5)  
  
    ReDim Ke(5)  
  
    ReDim Ce(5)  
  
    For j = 0 To 2  
  
        DOF(j) = True  
  
        Ce(j) = True  
  
    Next j  
  
    Ke(0) = Sheets("PANEL_INFO").Cells(8, 2).Value  
  
    Ke(1) = Sheets("PANEL_INFO").Cells(9, 2).Value  
  
    Ke(2) = Sheets("PANEL_INFO").Cells(10, 2).Value  
  
    Ce(0) = Ke(0)  
  
    Ce(1) = Ke(1)  
  
    Ce(2) = Ke(2)
```

```
ret = SapObject.SapModel.PropLink.SetLinear("L1", DOF, Fixed, Ke, Ce, 0, 0)
```

```
End Sub
```

```
Sub Sap2000_close()
```

```
'Close the SAP2000 application
```

```
SapObject.ApplicationExit False
```

```
'Set the objects to Nothing
```

```
Set SapObject = Nothing
```

```
Set coordinates = Nothing
```

```
End Sub
```